

2014

## Development of leaf shape and vein homologies in five species of the genus *Ipomoea* (Convolvulaceae)

Austin William Jones  
*University of Northern Iowa*

*Let us know how access to this document benefits you*

Copyright ©2014 Austin William Jones

Follow this and additional works at: <https://scholarworks.uni.edu/etd>



Part of the [Botany Commons](#), and the [Plant Biology Commons](#)

---

### Recommended Citation

Jones, Austin William, "Development of leaf shape and vein homologies in five species of the genus *Ipomoea* (Convolvulaceae)" (2014). *Dissertations and Theses @ UNI*. 326.

<https://scholarworks.uni.edu/etd/326>

This Open Access Thesis is brought to you for free and open access by the Student Work at UNI ScholarWorks. It has been accepted for inclusion in Dissertations and Theses @ UNI by an authorized administrator of UNI ScholarWorks. For more information, please contact [scholarworks@uni.edu](mailto:scholarworks@uni.edu).

**Offensive Materials Statement:** Materials located in UNI ScholarWorks come from a broad range of sources and time periods. Some of these materials may contain offensive stereotypes, ideas, visuals, or language.

Copyright by

AUSTIN W. JONES

2014

All Rights Reserved

DEVELOPMENT OF LEAF SHAPE AND VEIN HOMOLOGIES IN  
FIVE SPECIES OF THE GENUS *IPOMOEA* (CONVOLVULACEAE)

An Abstract of a Thesis  
Submitted  
in Partial Fulfillment  
of the Requirements for the Degree  
Master of Science

Austin William Jones  
University of Northern Iowa

May 2014

## ABSTRACT

Angiosperm leaves are extremely variable in form while predominantly maintaining the function of the primary photosynthetic organ of the plant. Changes in leaf form can result from myriad physiological processes which may be influenced by ecology, physical stimuli, phylogeny, or other factors. In studying the development of divergent leaf forms among closely related species, conserved morphological elements may be identified that are not apparent in the mature form. The genus *Ipomoea* (Convolvulaceae) contains over 600 species and a wide range in leaf shapes. Five species, *I. purpurea*, *I. coccinea*, *I. sloteri*, *I. quamoclit*, and *I. cairica* show a range in leaf forms from simple to highly dissected. Leaf development was tracked from initiation to maturity in order to identify how developmental trajectories diverge and what is conserved across species. Cleared leaf samples were analyzed and evidence was found supporting the homology between major vein patterns across species. Using these homologous veins, landmarks were established for morphometric analysis. A Generalized Procrustes Analysis was used on landmark coordinates and suggests, through Principal Components Analysis, that the shape described by major venation is conserved across these species despite major divergences in blade form.

DEVELOPMENT OF LEAF SHAPE AND VEIN HOMOLOGIES IN  
FIVE SPECIES OF THE GENUS *IPOMOEA* (CONVOLVULACEAE)

A Thesis  
Submitted  
in Partial Fulfillment  
of the Requirements for the Degree  
Master of Science

Austin William Jones  
University of Northern Iowa  
May 2014

This Study by: Austin William Jones

Entitled:

Development of Leaf Shape and Vein Homologies in Five Species of the Genus

*Ipomoea* (Convolvulaceae)

has been approved as meeting the theses requirement for the

Degree of Master of Science

---

Date

---

Dr. Julie Kang, Chair, Thesis Committee

---

Date

---

Dr. Steve L. O’Kane Jr., Thesis Committee Member

---

Date

---

Dr. Marek Sliwinski, Thesis Committee Member

---

Date

---

Dr. Michael J. Licari, Dean, Graduate College

## ACKNOWLEDGMENTS

I would like to recognize those whose contribution of time, effort, and insight were crucial in the completion of this work. Foremost, I would like to thank my advisor and committee chair Dr. Julie Kang for her continued guidance through the organization, experimentation, and interpretation involved in this study and the ultimate composition of this text. The remaining members of my thesis committee, Dr. Steve O'Kane and Dr. Marek Sliwinski also gave valuable time and energy in ensuring the validity of this work and their contributions are greatly appreciated. The members of the Dr. Neelima Sinha laboratory at UC-Davis also donated time and expertise, as well as laboratory space, in order to personally assist me. Their technical help, particularly from Dr. Daniel Chitwood with landmark-based morphometrics, provided an essential knowledge base without which this work would not have been possible. For making this collaboration possible, I would also like to thank the microMORPH Research Coordination Network. Finally, I was able to build a better context for this work thanks to Dr. Jim Solomon, who granted me access to the Missouri Botanical Garden Herbarium so that I could photograph and document collected samples of *Ipomoea*.

## TABLE OF CONTENTS

	PAGE
LIST OF TABLES.....	v
LIST OF FIGURES.....	vi
CHAPTER 1. INTRODUCTION.....	1
CHAPTER 2. MATERIALS AND METHODS.....	15
Plant Material .....	15
Scanning Electron Microscopy.....	15
Light Microscopy .....	16
Morphometric Analysis .....	17
CHAPTER 3. RESULTS.....	19
Leaf Development.....	19
Vein Homology .....	30
Morphological Analysis .....	43
CHAPTER 4. DISCUSSION.....	57
REFERENCES.....	69
APPENDIX. HERBARIUM LEAF SAMPLES .....	84

## LIST OF TABLES

TABLE	PAGE
1 P-values from Pairwise t-test of Means Along PC1 .....	47
2 P-values from Pairwise t-test of Means Along PC2 .....	48
3 P-values from Pairwise t-test of Means Along PC3 .....	50
4 P-values from Pairwise t-test of Means Along PC4 .....	52
5 P-values from Pairwise t-test of Means Along PC5 .....	54
6 P-values from Pairwise t-test of Means Along PC6 .....	56

## LIST OF FIGURES

1	Mature Leaf Shape of Each Species .....	20
2	Leaf Development in <i>I. pupurea</i> .....	21
3	Leaf Development in <i>I. coccinea</i> .....	23
4	Leaf Development in <i>I. sloteri</i> .....	26
5	Leaf Development in <i>I. quamoclit</i> .....	28
6	Leaf Development in <i>I. cairica</i> .....	29
7	Vascular Strand Differentiation in <i>I. pupurea</i> .....	32
8	Vascular Strand Differentiation in <i>I. coccinea</i> .....	35
9	Vascular Strand Differentiation in <i>I. sloteri</i> .....	37
10	Vascular Strand Differentiation in <i>I. quamoclit</i> .....	38
11	Vascular Strand Differentiation in <i>I. cairica</i> .....	40
12	Procrustes Landmarks Plotted on Mature Leaves of Each Species .....	43
13	Species Landmarks After Scaling and Rotation .....	45
14	PC1 Describing 59.6% of Total Shape Variation.....	47
15	PC2 Describing 17.4% of Total Shape Variation.....	48
16	PC3 Describing 8.8% of Total Shape Variation.....	50
17	PC4 Describing 8.4% of Total Shape Variation.....	52

18 PC5 Describing 3.6% of Total Shape Variation.....	54
19 PC6 Describing 2.7% of Total Shape Variation.....	56

## CHAPTER 1

### INTRODUCTION

Angiosperm leaves show a remarkable diversity in form, despite sharing the function of the primary photosynthetic organ. Due to the plasticity of leaf shape in response to numerous genetic and environmental effects, wide ranges in leaf form may be seen within closely related taxa, across populations, and even in the heteroblasty of individual plants. Many current studies have focused either on across-population variation in model species or on widely ranging taxa across angiosperms (Bharathan et al. 2002; Geeta et al. 2012; Kim, McCormick, et al. 2003; Klingenberg et al. 2012; Perez-Perez et al. 2011). There have been few, however, that have investigated the development of highly divergent leaf shapes between closely related species (Barth et al. 2009; Gleissberg 2004; Gleissberg 1998; Gleissberg and Kadereit 1999; Groot et al. 2005; Nicotra et al. 2011). The expression patterns and dramatic influences of the major determinants of leaf shape have been uncovered, including *KNOTTED1*-like *HOMEODOMAIN* (*KNOX1*) genes, *PINFORMED1* (*PIN1*) (auxin) genes, *CUP-SHAPED COTYLEDONS* (*CUC*) genes, as well as the HD-ZIP III gene family: *KANADI*, *YABBY*, *PHANTASTICA* (*PHAN*) and orthologous genes (Bilsborough et al. 2011; Bowman 2000; Canales et al. 2010; Champagne and Sinha 2004; Emery et al. 2003; Eshed et al. 2004; Hay

and Tsiantis 2010; Ilegems et al. 2010; Kim, McCormick, et al. 2003; McConnell 2001; Piazza et al. 2010; Siegfried et al. 1999; Tsukaya 2005; Vlad et al. 2014; Waites and Hudson 1995; Waites et al. 1998). Independent aspects of mature form, though, can conceivably be determined by more subtly expressed factors, like *MIR164a*, an indirectly induced miRNA which affects levels of CUC expression (Hasson et al. 2011; Nikovics et al. 2006; Peaucelle et al. 2007; Spinelli et al. 2011). Also, selective forces likely act on one or more of these determinants independently, rather than on all the processes that determine leaf shape as a whole (Jones et al. 2009). Alternatively, aspects of final leaf form can be the result of pleiotropy, as is the case in tomato and *Alstroemeria psittacina* Lehm., in both of which it was found that inherent left-right asymmetry in the leaf was a remnant of the auxin transport pattern in the meristem and young shoot that produced the spiral phyllotaxis (Chitwood, Headland, Ranjan, et al. 2012; Chitwood, Naylor, et al. 2012). Comparing the divergent morphological development among closely related species may point to conserved structural patterns that reflect the common ancestry of the group. Furthermore, determining when and how developmental plans diverge will shed light on differing patterns of gene expression, which will help to build a foundation for

future studies focused on elucidating how spatiotemporal changes in developmental regulatory processes have changed over evolutionary time.

The development of leaf form begins, as with all lateral organs, from the shoot apical meristem (SAM), a dome-shaped region of pluripotent cells which generates the entire above-ground biomass of the plant. For the duration of vegetative growth, the SAM retains indeterminacy and exhibits rapid cell division as lateral organs arise as primordia from the flanks of the SAM. Leaf initiation occurs this way as initial cells are designated within the SAM flank and subsequently divide outward to form a rounded protrusion, the leaf primordium. The identity of the leaf primordium, along with maintenance of indeterminacy in the rest of the SAM is largely mediated by changes in the expression of *KNOTTED1*-like *HOMEODOMAIN* (*KNOX*) genes (Champagne and Sinha 2004; Efroni et al. 2010; Hay and Tsiantis 2010; Jackson et al. 1994; Kerstetter et al. 1997; Long, Moan et al. 1996; Sinha et al. 1993; Smith et al. 1992; Vollbrecht et al. 1990), as well as directed transport and response to the phytohormone auxin (Fleming et al. 1993; Koenig et al. 2009; Kuhlemeier et al. 1993; Mattsson et al. 2003; Nakayama and Kuhlemeier 2009; Reinhardt et al. 2000; Stieger et al. 2002). In the angiosperm lineage, members of the *KNOX* family are required for maintenance of SAM indeterminacy, with leaf primordium initiation

at the SAM flank involving a characteristic decrease in KNOX expression (Hay and Tsiantis 2010; Janssen, Lund, and Sinha 1998; Jasinski et al. 2007; Long, McConnell, et al. 1996; Ori et al. 2000; Sousa-Baena et al. 2014). This designation of leaf cell initials is simultaneously correlated with a convergence of auxin flow, directed by the polar expression of the auxin efflux carrier PIN1 (Bayer et al. 2009; Benkova et al. 2003; Chen et al. 2013; Galweiler et al. 1998; Hay and Tsiantis 2010; Koenig et al. 2009; Kuhlemeier and Reinhardt 2001). This function is exemplified in *Arabidopsis*, in which *pin1* mutants fail to initiate lateral organs (Hay and Tsiantis 2010; Kuhlemeier and Reinhardt 2001; Reinhardt et al. 2003; Reinhardt et al. 2000), and in maize, in which apices grown in the presence of an auxin transport inhibitor exhibit the same phenotype (Scanlon 2003, Tsiantis et al. 1999). In most simple-leaf taxa studied, including *Arabidopsis*, maize, tobacco, and snapdragon, KNOX expression is down-regulated for the duration of leaf development (Champagne and Sinha 2004; Hay and Tsiantis 2009; Kim, Yuan, and Jackson 2003; Koltai and Bird 2000; McHale and Koning 2004; Scanlon 2000; Zoulias et al. 2012). In most compound leaves as well as some lobed and serrated leaves, however, expression reappears in leaf primordia and is necessary for the development of leaflets and lobing (Bharathan et al. 2002; Burko and Ori 2013; David-Schwartz et al. 2009; Kim, Pham, et al. 2003; Shani et

al. 2009). The re-expression of KNOX creates a state of transient indeterminacy in the primordium, which allows for the elaboration of marginal outgrowths (Barth et al. 2009; Groot et al. 2005; Hagemann and Gleissberg 1996). Exceptions to this have been described in pea (Champagne et al. 2007) where KNOX function is replaced by UNIFOLATA (DeMason and Chawla 2004; DeMason and Chetty 2011; Gourlay et al. 2000; Hofer et al. 1997), and in the palm *Chamaedorea elegans* Mart., where compounding is achieved through the mechanical separation of plications during secondary morphogenesis (Kaplan et al. 1982; Nowak et al. 2011). The presence or absence of marginal outgrowths in the primordium is also affected by patterns of auxin accumulation (Ben-Gera et al. 2012; Ben-Gera and Ori 2012; Berger et al. 2009, Bilsborough et al. 2011; David-Schwartz et al. 2009; Koenig et al. 2009). These marginal outgrowths result from the formation of auxin maxima along the margin, similar to that which initiates the primordium itself from the SAM, while simple leaves show relatively uniform concentrations of auxin along the margin (Ben-Gera et al. 2012; Hay et al. 2006; Koenig et al. 2009). The degree to which auxin transport and KNOX expression affect one another during leaf development has been investigated in *Arabidopsis* (Burko and Ori 2013; David-Schwartz et al. 2009; Hay et al. 2006; Perez-Perez et al. 2011; Scanlon 2003), where it was shown that PIN1-mediated

auxin fluxes are necessary to repress the KNOX gene *BREVIPEDICELLUS* (*BP*) at leaf initiation, and that ectopic KNOX expression in the leaf disrupts PIN1-directed auxin gradients, resulting in marginal outgrowths (Belles-Boix et al. 2006; Hay et al. 2006; Grigg et al. 2005; Mele et al. 2003; Venglat et al. 2002). Thus, patterns of KNOX expression and auxin transport are pervasive and critical in determining leaf initiation, as well as the presence and placement of marginal outgrowths which will result in lobes and/or leaflets.

In any context with regard to molecular determinants, mature leaf form must be determined by the presence or absence of primordium outgrowths and the degree to which the leaf margins remain indeterminate. Closely related species will presumably share some patterns in leaf development such as heteroblasty, patterns of leaf marginal outgrowth, or unique genetic pathways. For example, species in *Lepidium* show remarkable similarities in leaf form until late in development, when simple forms diverge from dissected forms via differential expansion in secondary morphogenesis (Bharathan et al. 2002). Another example is the genus *Ampelopsis*, in which divergent forms are apparent early in development, but similar patterns of repeated acropetal initiation of outgrowths, points to likely homologies in the leaf developmental plan, reflecting the recent common ancestry of the clade (Jones et al. 2013). A unique

genetic pathway involving members of FLORICULA/LEAFY (FLO/LFY), which function in floral meristem maintenance, controls compound leaf development in a large subclade of the Fabaceae (Champagne et al. 2007), but has not been found elsewhere in the angiosperms with similar function. Common developmental patterns are often found across closely related species, and this is combined with the possibility for individual aspects of leaf form to evolve at different rates (Jones et al. 2009, Spinelli et al. 2011) in response to myriad environmental factors (Chitwood, Headland, Foliault, et al. 2012). This allows the homology of anatomical, morphological, and genetic factors in development to be investigated in the context of wide ranging morphologies across a clade with many possible causes for the variation.

Leaf vein differentiation is another integral part of establishing mature leaf form. Venation must coincide closely with the specific developing leaf form to ensure optimal transport of solutes and photosynthetic products. Angiosperm leaves have adopted a reticulate vein pattern, formed hierarchically, in order to facilitate this transport by maximizing the vein density relative to laminar tissue (Dengler and Kang 2001; Kang and Dengler 2005; Nelson and Dengler 1997; Nicotra et al. 2011; McKown et al. 2010; Sack and Scoffoni 2013; Scoffoni et al. 2011). Like primordium outgrowths and the initiation of the primordium itself,

vein differentiation follows patterns of auxin transport (Dengler and Kang 2001; Kang and Dengler 2002; Kang and Dengler 2004; Mattsson et al. 2003; Scarpella et al. 2006; Scarpella et al. 2010). The convergence of auxin flow at the site of primordium initiation, mediated by polar PIN1 expression, results in a maximum of auxin concentration at the primordium tip (Bayer et al. 2009; Koenig et al. 2009; Mattsson et al. 2003; Nakayama and Kuhlemeier 2009; Reinhardt et al. 2003; Scarpella et al. 2010). The process of acquiring procambial identity then begins as PIN-1 expression directs auxin transport from the margin medially and basally (Bilsborough et al. 2011; Garrett et al. 2012; Koenig et al. 2009; Mattsson et al. 2003; Sawchuk et al. 2013; Scarpella et al. 2010; Wenzel et al. 2007). This occurs somewhat diffusely and provides a background from which preprocambial cell files (precursor cells of procambium) will be selected (Donner et al. 2010; Donner et al. 2009; Scarpella et al. 2010; Scarpella et al. 2004). The acquisition of preprocambial identity, defined in *Arabidopsis* by AtHB-8 (*ARABIDOPSIS THALIANA HOMEBOX GENE-8*) expression, progresses continually either laterally from the midvein or proximally from existing marginal veins (Baima et al. 2001; Donner et al. 2009; Donner et al. 2010; Gardiner et al. 2011; Kang and Dengler 2002; Scarpella et al. 2010). With this background in place, procambial strands often appear simultaneously along their entire

length of the preprocambial strand (Kang and Dengler 2004; Sawchuck et al. 2007; Scarpella et al. 2010; Scarpella et al. 2004), forming loops connecting to existing strands, tapering and terminating within the blade, or terminating at the margin (Roth-Nebelsick A 2001). Higher-order connecting veins develop in a similar fashion as PIN-1 files arise between existing veins, resulting in the dense reticulate vascular network that is characteristic of angiosperms (Scarpella et al. 2010). Thus, the formation of veins occurs hierarchically in response to polar auxin transport, an idea supported by observation of leaves grown in the presence of auxin transport inhibitors, in which vein differentiation is localized to the leaf tip and margins only (Mattsson et al. 2003; Mattsson et al. 1999; Wenzel et al. 2007). In this scenario, auxin is prevented from draining towards pre-existing vasculature through sub-epidermal tissues, effectively inhibiting the midvein and secondary veins from forming (Mattsson et al. 2003; Mattsson et al. 1999; Wenzel et al. 2007). Unique leaf shapes present across taxa, therefore, could presumably exhibit unique patterns of auxin transport and accumulation which result in the varying vein patterns that supply them. Alternatively, likely homologous elements of vein pattern in divergent forms from closely related species, like the prominent secondary veins of *Ampelopsis cordata* Michx. and

*Ampelopsis arborea* (L.) Koehne (Jones et al. 2013), could point to conserved patterns of auxin transport and response within a clade.

The genus *Ipomoea*, the largest in the Convolvulaceae (morning glory family), consists of over 600 species with worldwide distribution (Baucom et al. 2011; Miller et al. 2004; Manos et al. 2001), and is placed sister to the Solanaceae in the Solanales (Stefanovic et al. 2002). Stefanovic et al. (2002) found evidence for the monophyly of the Convolvulaceae, including *Cuscuta*, tribe Dichondreae, and *Humbertia*. The inclusion of these three groups, as described, into a monophyletic Convolvulaceae had previously been uncertain (Stefanovic et al. 2002). However, the delimitation of monophyletic groups within the family has proved difficult, particularly those which correspond to the traditional description of groups based on morphology (Stefanovic et al. 2002, Manos et al. 2001). Substantive evidence has also been found for the polyphyly of *Ipomoea*, with molecular phylogenetic reconstructions failing to separate the group completely from closely related genera (Manos et al. 2001, Stefanovic et al. 2002). Despite this uncertainty in convolvulaceous genus-level delimitations, *Ipomoea* presents an interesting model for evolutionary study. Baucom et al. (2011) argue that characteristics of the genus, such as wide ranging ecological situations and mating systems, the importance of the genus as both a crop and a noxious weed,

and common growth habit characterized by fast rates of growth and reproduction, make the genus an optimal model for future genetic and evolutionary study. Included in the generic morphological diversity is leaf form, with species exhibiting a wide range from simple and entire to highly dissected to compound. Furthermore, evidence was found for selection acting on leaf shape alleles in *I. hederacea*, in which distinct shapes are separated by latitude (Bright and Rausher 2008; Campitelli and Stinchcombe 2013a). Experimentally applied pressures were unable, however, to produce significant differences in fitness between leaf shapes (Baucom et al. 2011; Campitelli et al. 2013; Campitelli and Stinchcombe 2013b).

A Generalized Procrustes Analysis (GPA) is normally used on raw shape data, either 2- or 3-dimensional, in order to remove size and degree of rotation from consideration so that only differences in shape between samples are being considered during interpretation. When analyzing leaf shape in this way, usually either landmarks are assigned to predetermined points on the sample leaves, the landmark point values being subject to the analysis (Viscosi and Cardini 2011), or the continuous leaf margin is estimated by tools like elliptic Fourier descriptors (Chitwood, Headland, Kumar, et al. 2012). Landmark data were used here to estimate the vein tip positions of the common vein pattern. In

this type of 2-dimensional shape analysis, coordinate point values are assigned to each of the chosen landmarks for each sample. In the GPA, shape is normalized from the raw data by normalizing the centroid size of all samples. Differences between samples in translation and rotation are minimized by a least-squares algorithm. The result is a dataset of landmark shapes without size, rotational, or translational differences that can be analyzed statistically in order to determine patterns of variation in shape only.

The tool used to analyze Procrustes shape variation here was Principal Components Analysis (PCA), a statistical analysis used for the interpretation of high-dimensional data sets. In data sets with increasing number of variables, it becomes essentially impossible to simply plot variables against each other graphically. In order to discern which variables, out of many, most affect the overall variation seen in the dataset, PCA is commonly used. With a dataset in  $n$ -dimensional space, PCA works by projecting orthogonal vectors which span the variance of the data, the principal components (PCs). The first PC maximizes the amount of variance that can be explained by a vector and, therefore, explains the highest percentage of the total variance of all PCs. The second PC maximizes the percentage of variance that can be explained along a vector that is orthogonal to the first PC, and therefore explains the second highest percentage of the total

variance. This continues until the entire variation within the dataset has been accounted for, resulting in a number of PCs that is less than or (usually) equal to the number of dimensions. After identifying how many PCs account for a significant percentage of the total variation, each can be visualized graphically or otherwise compared to the data so that which variables contribute most to the variation described along the given PC can be identified. In this way, the variables which most affect the total variation seen and which are less influential can be identified in high-dimensional datasets with which direct graphical representation is not possible.

Given the potential of leaves as a model of variable and dynamic developmental morphology and related genetics and physiology, we describe the morphological leaf development of five species within a genus, *Ipomoea*, that represent a range of mature leaf shapes. As well resolved and comprehensive species-level phylogenetic relationships in the genus are lacking, the study group was selected to represent a range in leaf forms, rather than specific intra-generic groups. Leaf shapes in the study group include simple and entire (*I. purpurea* (L.) Roth), simple with a serrated margin (*I. coccinea* L.), lobed with increasingly dissected margins (*I. sloteri* (House) van Ooststr. and *I. quamoclit* L.), and palmately compound (*I. cairica* (L.) Sweet). This provides the potential, with

closely related but morphologically different species, to better understand how divergent forms are acquired through development and to recognize common growth patterns that could reflect common ancestry. Despite the range in leaf forms, all five species exhibit pairs of secondary major veins arising from the petiole-blade junction. Along with when and how morphologies diverge during development, a combination of microscopic techniques were used to investigate the hypothesis that this vein pattern is homologous across these species. The pattern of vasculature that is understood to be homologous across species was then used to establish landmarks for morphometric shape analysis. Finally, landmark point values were used to perform a Generalized Procrustes Analysis (GPA), followed by a Principal Components Analysis (PCA) to interpret the data and to extract conclusions about how the shape defined by this common vein pattern varies, if at all, between species.

## CHAPTER 2

### MATERIALS AND METHODS

#### Plant Material

All plant material was grown from seed under identical conditions, in Conviron Adaptis A1000 growth chamber (Conviron, Pembina, North Dakota, USA) at 22°C, 50 percent humidity, and light intensity level 1. Seed coats were cut at the hilum end and soaked in 10N sulfuric acid for one hour. Seeds were then rinsed with distilled water and plated on filter paper in petri plates, filled to half of seed height with distilled water. Plates were covered with aluminum foil and left at room temperature to germinate. Germinating seeds were checked daily and sown onto soil at the emergence of the radicle. Seeds were sown into general purpose potting soil in 2" pots and pots were placed in flats, watered from the bottom, domed, and placed in the growth chamber. Domes were removed at the emergence of cotyledons and plants were allowed to grow freely, watering once every three days with a 1:4 fertilizer:diH<sub>2</sub>O diluted fertilizer (24-8-16 N-P-K) solution.

#### Scanning Electron Microscopy

Scanning electron microscopy was conducted on shoot tips from approximately 20 individuals for each species. Tissue was fixed in FAA

(formalin:glacial acetic acid:70% ethanol, 9:1:1) overnight, dehydrated through an ethanol series, and critical point dried with CO<sub>2</sub> on a Tousimis Samdri-795 (Tousimis, Rockville, Maryland, USA). Samples were Sputter Coated with a Cressington 108 Auto Sputter Coater (Watford, England) and viewed at 20 kV with a Tescan Vega 5136 Scanning Microscope (Cranberry Township, Pennsylvania, USA). Images were captured digitally using the Vega TC software (Tescan USA Inc., Cranberry Twp, Pennsylvania, USA).

#### Light Microscopy

Shoot tips and young leaves of all species were collected and boiled in 70% EtOH until all chlorophyll was removed. Samples were transferred to saturated chloral hydrate (Sigma, St. Louis, Missouri, USA) and kept at room temperature, at least overnight, until cleared. Shoot apices and young leaves were mounted on slides in a 1:1 glycerol:chloral hydrate solution. Fresh material and material stored in 70%EtOH were also collected for imaging. Images were viewed on a Zeiss Discovery V.12 SteREO microscope, with images taken on a Zeiss AxioCam and visualized in ZEN (Carl Zeiss MicroImaging GmbH, USA). Images were digitally processed in Adobe Photoshop CS5 Extended® (Adobe Systems Inc., San Jose, California, USA).

### Morphometric Analysis

The fifth leaf along the main stem was selected for morphometric analysis. Leaves were collected after full expansion, determined by first appearance of signs of senescence at the leaf tip. Leaf samples were placed on a light table, adaxial face down, and flattened with a glass pane. Samples were then photographed by a digital camera mounted at 10 inches above the sample on a camera mount. Digital leaf images were uploaded into ImageJ ([imagej.nih.gov/ij/](http://imagej.nih.gov/ij/)), where landmark plotting was performed. A total of 311 leaf samples were collected for analysis: 48 for *I. purpurea*, 46 for *I. coccinea*, 59 for *I. sloteri*, 113 for *I. quamoclit*, and 45 for *I. cairica*.

Six landmarks were chosen based on the two pairs of secondary major veins common to all species, as well as both ends of the midvein. In species with dissected leaves (*I. sloteri*, *I. quamoclit*, and *I. cairica*), landmarks 3-6 corresponding to secondary major veins were placed at vein tips. In species with simple leaves (*I. purpurea* and *I. coccinea*), vein trajectories were extended from the petiole-blade junction and landmarks were placed at the intersection of the extended trajectory and the blade margin. As such, landmark 1 was placed at the petiole-blade junction, landmark 2 at the tip of the midvein, landmark 3 at the right proximal secondary vein tip or extended trajectory, landmark 4 at the right

distal secondary vein tip or extended trajectory, landmark 5 at the left distal secondary vein tip or extended trajectory, and landmark 6 at the left proximal secondary vein tip or extended trajectory. Landmarks were plotted onto digital leaf images in ImageJ ([imagej.nih.gov/ij/](http://imagej.nih.gov/ij/)), after scaling, and coordinates for each landmark were recorded.

Raw coordinate landmark values were used for Generalized Procrustes Analysis (GPA) in R ([www.r-project.org](http://www.r-project.org)). Coordinate values were imported and the GPA() function, in the 'shapes' package in R ([www.r-project.org](http://www.r-project.org)), was used to run the Generalized Procrustes and subsequent Principal Components Analysis. Graphical results were obtained using the 'ggplot2' package.

## CHAPTER 3

### RESULTS

#### Leaf Development

Leaf development in each species was tracked from initiation to maturity via scanning electron microscopy (SEM) and light microscopy. In each species, leaves are initiated spirally from the shoot apical meristem (SAM) and are first evident as rounded primordia. Primordia will be numbered here such that the youngest primordium visible represents the primordium 1 (P1) stage, transitioning into the P2 stage when the next primordium becomes visible and is the new P1.

#### *I. purpurea*

The mature leaf shape of *I. purpurea* is simple and entire, with a cordate base and acuminate tip (Fig 1A). P1 primordia are first visible as rounded protrusions from the flank of the SAM (Fig 2A). As the P1 stage progresses into P2 and P3, the primordium elongates and widens basally (Fig 2A). Also at this stage, as the primordium elongates, the distal end (leaf tip) begins to re-curve, effectively preventing direct contact with adjacent primordia (Fig 2A-D). During late P3 and into P4, trichomes are initiated on both adaxial and abaxial sides of the primordium (Fig 2A-B). Through successive stages, abaxial trichomes

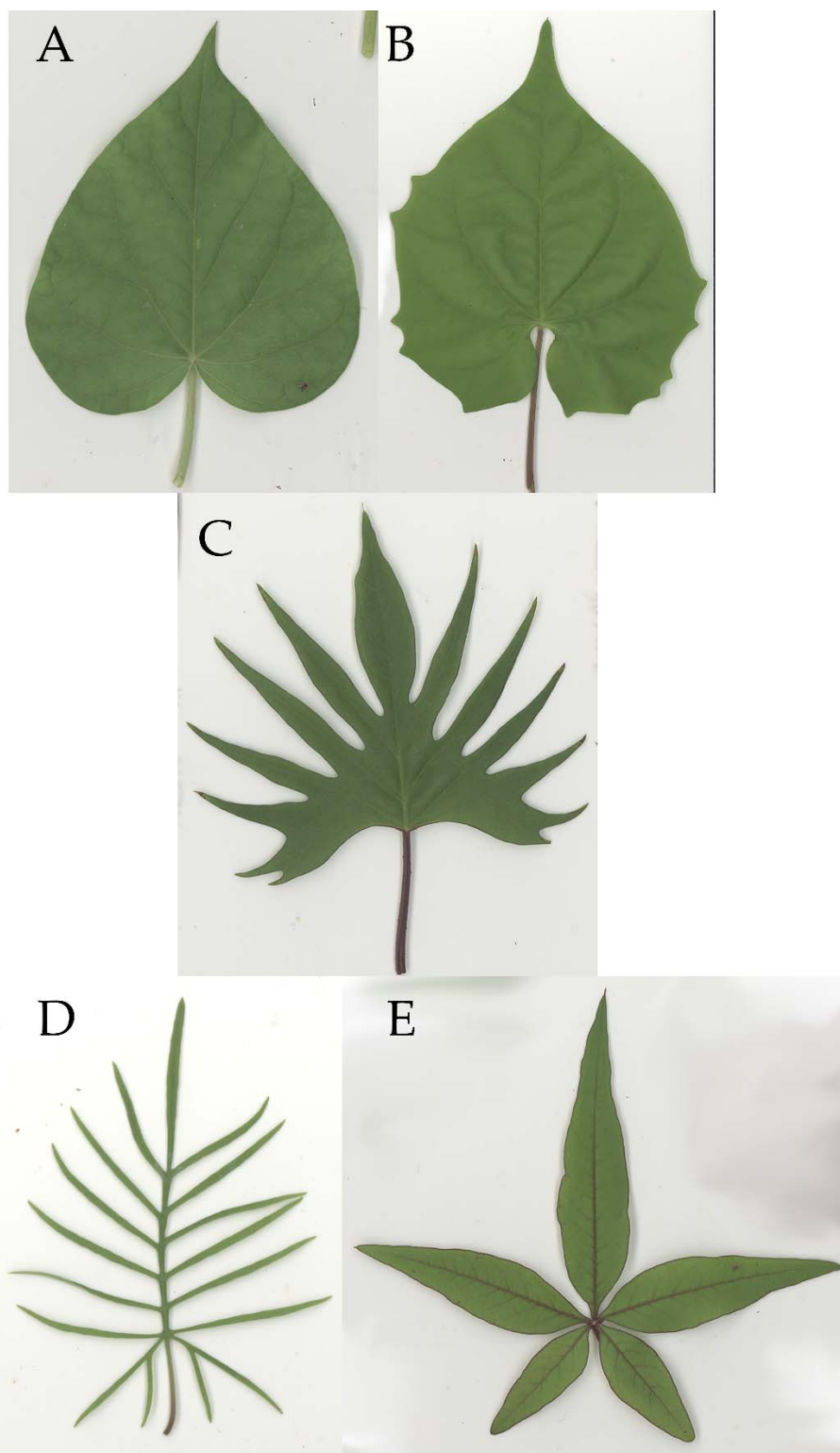


Figure 1. Mature Leaf Form of Each Species. (A) *I. purpurea*. (B) *I. coccinea*. (C) *I. sloteri*. (D) *I. quamoclit*. (E) *I. cairica*.

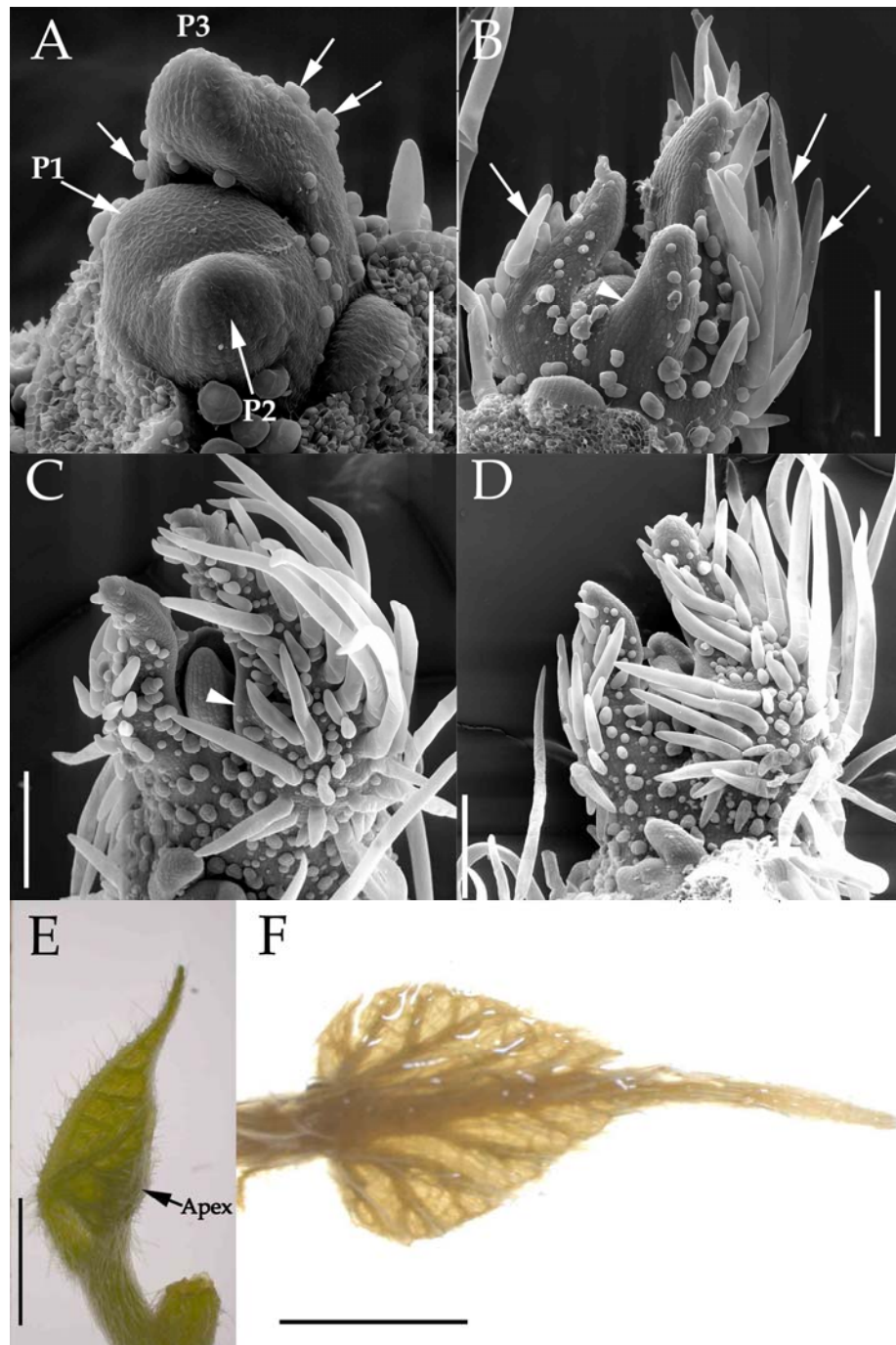


Figure 2. Leaf Development in *I. purpurea*. (A-D) SEM images of developing primordia. (A) P1-P3 stages with trichomes visible at P3. (B-D) Successive primordium stages showing marginal expansion and trichome outgrowth. (E) Young leaf folded around the apex. (F) Young unfolded leaf. Scale Bars: (A) 100 $\mu$ m. (B-D) 200 $\mu$ m. (E-F) 3mm. Expanding primordia margins (arrowheads). Trichomes (arrows).

become denser and quickly elongate so that the entire primordium is soon encompassed (Fig 2C-D). Simultaneous with this trichome development, blade expansion becomes apparent as the margins begin to expand along either side of the SAM (Fig 2B, arrowhead). With the margin remaining entire and bilaterally folded, growth continues throughout progressive stages to envelope the apex (Fig 2C-E). The mature leaf form becomes apparent, as the proximal lamina expands more rapidly and becomes recognizable as the cordate leaf base (Fig 2C, arrowhead). The young leaf remains folded about the apex until relatively late in development when the leaf is ~7-8mm (Fig 2E). Complete unfolding occurs when the leaf is ~9-10mm and moves away from the apex (Fig 2F). The rest of development is characterized by further expansion, resulting in the mature leaf form (Fig 1A).

### *I. coccinea*

The mature leaf shape of *I. coccinea* is simple, with a dentate margin, deeply cordate base and acuminate tip (Fig 1B). Primordia are initiated as rounded protrusions from the flank of the SAM (Fig 3A). Through the P2 and P3 stages, the primordium widens basally and progressively separates from the SAM (Fig 3A-B). Also during this stage, the leaf margins begin expanding along the

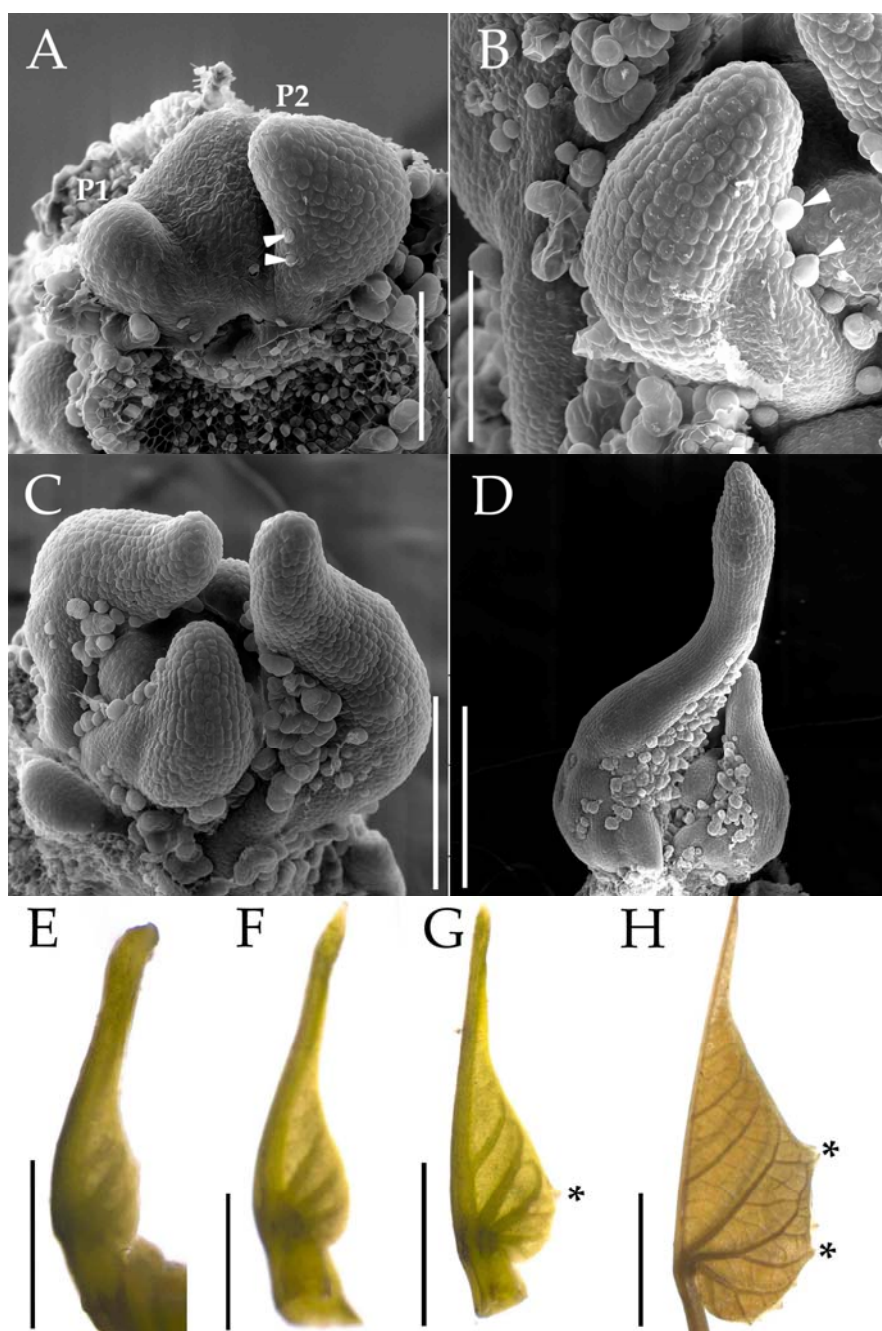


Figure 3. Leaf Development in *I. coccinea*. (A-D) SEM images depicting early leaf development. (A) P1 and P2 stages. (B) Early P-stage showing expanding margins with developing trichomes. (C-D) Later P-stages (~P4-P7) showing continued leaf elongation and trichome development. (E-H) Young leaf samples depicting blade expansion and appearance of serrations. Scale Bars: (A-B) 100 μm. (C) 200 μm. (D) 400 μm. (E-F) 1 mm. (G) 2 mm. (H) 4 mm. Trichomes (arrowheads). Marginal teeth (asterisks).

proximal region of the primordium (Fig 3B). Trichomes are initiated along the margins beginning in P1 and continuing as the margins begin to flatten and expand through late P2 and into P3 (Fig 3A-B, arrowheads). As development continues through successive stages (~P4 – P7), leaf elongation continues along the proximal-distal axis and primordia begin to re-curve at the distal tip, effectively avoiding direct contact with adjacent primordia (Fig 3C). Also during these stages, trichome initiation continues to be localized near the expanding margins, so that dense trichome cover is soon evident across the expanding blade, but is almost absent elsewhere on the primordium (Fig 3C-D). Successive stages are characterized by further blade expansion and elaboration of the mature leaf form (Fig 3E-G). The marginal serrations present in the mature leaf are not apparent until relatively late in development when the leaf is ~4-5mm, after considerable blade expansion but before unfolding (Fig 3F-G, asterisks). Unfolding of the lamina occurs after the young leaf (~15-20mm) is no longer in the vicinity of the apex, and expansion continues until mature form is reached (Fig 1B).

### *I. sloteri*

The mature leaf of *I. sloteri* has a smooth but deeply lobed margin (Fig 1C). Leaf primordia are initiated as rounded protrusions from the flank of the SAM

(Fig 4A-B). Through P1 and P2, the primordium quickly assumes an arched posture over the SAM flank from which it arose (Fig 4A-B). As late P2 transitions into P3, the base of the primordium progressively separates from the flank of the SAM, while the primordium continues to elongate along the proximal-distal axis and bend over the SAM (Fig 4A-B). Starting in late P3 and progressing into P4, trichomes are initiated along the primordium margins (Fig 4A-B, arrowheads). Shortly thereafter, marginal lobes are initiated basipetally inside the line of marginal trichomes and quickly begin to extend (Fig 4C-D, arrows). Trichome density will remain greatest in areas of lobe outgrowth and lesser in sinuses (Fig 4D-E). By this stage, there are 4-8 lobe pairs and the marginal lobes undergo extensive elongation (Fig 4E). Also, the distal ends of the primordia remain bent over the apex so that the distal end of a primordium projects directly over that of the adjacent younger primordium (Fig 4E). The most proximal lobes, and therefore the last lobes to develop, are not as deeply dissected as distal lobes (Fig 4G). Lamina expansion proceeds along through successive young leaf stages as the leaf remains folded (Fig 4E-G). The young leaf begins to unfold when the leaf is ~5mm (Fig 4H), and becomes completely unfolded as it approaches mature form (Fig 1C).

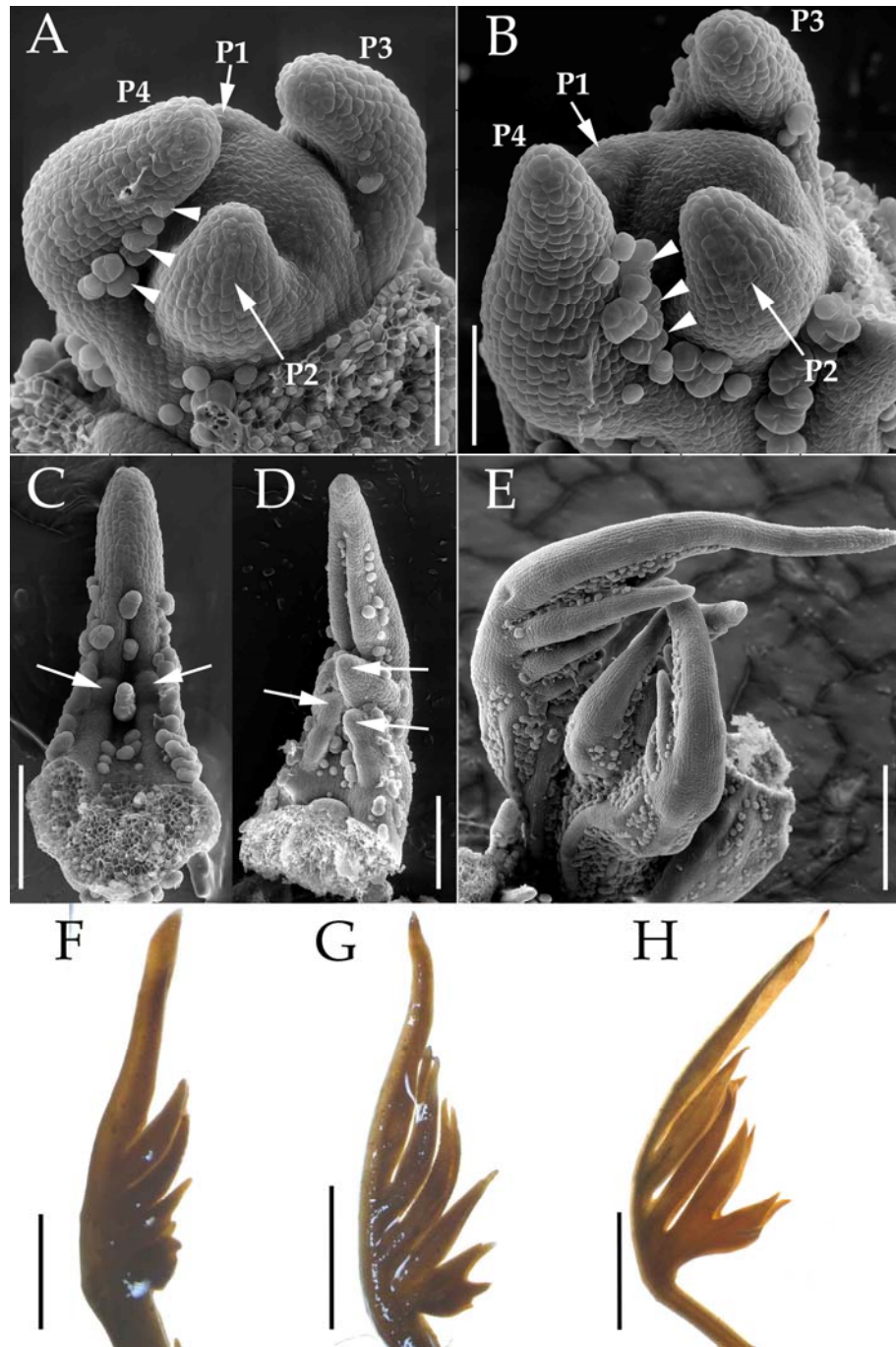


Figure 4. Leaf Development in *I. sloteri*. (A-E) SEM images depicting early stages of leaf development. (A-B) P1-P4 stages. (C-D) Initiation and early elongation of marginal lobes. (E) Later primordium-stages (~P6-P9) showing elongated lobes and terminal lobe arching over the apex. (F-H) Young leaf samples depicting lobe elongation and blade expansion. Scale Bars: (A-B) 100 $\mu$ m. (C-D) 200 $\mu$ m. (E) 500 $\mu$ m. (F-G) 1mm. Trichomes (arrowheads). Marginal lobes (arrows).

*I. quamoclit*

The mature leaf form of *I. quamoclit* consists of a smooth but deeply (nearly to the midrib) dissected margin producing very narrow pinnate lobes (Fig 1D). Leaf primordia are initiated as rounded protrusions from the flank of the SAM (Fig 5A). Beginning at P4, trichomes are initiated along the primordium margins (Fig 5A-D, arrowheads). Marginal lobes begin to appear late in development at approximately P8 (Fig 5C-D, arrows). Marginal trichomes remain sparse through this period (Fig 5C-D). The full complete set of marginal lobes are present when the leaves are ~2.5mm (Fig. 5E-G). Successive stages of leaf development are characterized by extensive outgrowth of the lobes accompanied by only a small amount of blade expansion on each lobe resulting in filamentous lobes (Fig 5F-H). The leaf becomes completely unfolded (~12mm) as it approaches the fully expanded mature form (Fig 1D).

*I. cairica*

The mature leaf form of *I. cairica* is deeply lobed into five palmate laminar units with smooth margins (Fig 1E). Although deeply lobed, laminar units are not completely separate and the leaf is not fully compound. Leaf primordia are initiated as rounded protrusions from the flank of the SAM (Fig 6A-B). At primordium 3, the base of the primordium widens as the leaf margins become



Figure 5. Leaf Development in *I. quamoclit*. (A-D) SEM images depicting early stages in leaf development. (A-B) P1-P4 stages. (C-D) Later primordium stages with marginal lobe initiation. (E-H) Young leaves with the full complement of marginal lobes. Scale Bars: (A-B) 100. (C-D) 200. (E) 1mm. (F) 2mm. (G) 3mm. (H) 4mm. Trichomes (arrowheads). Marginal lobes (arrows).

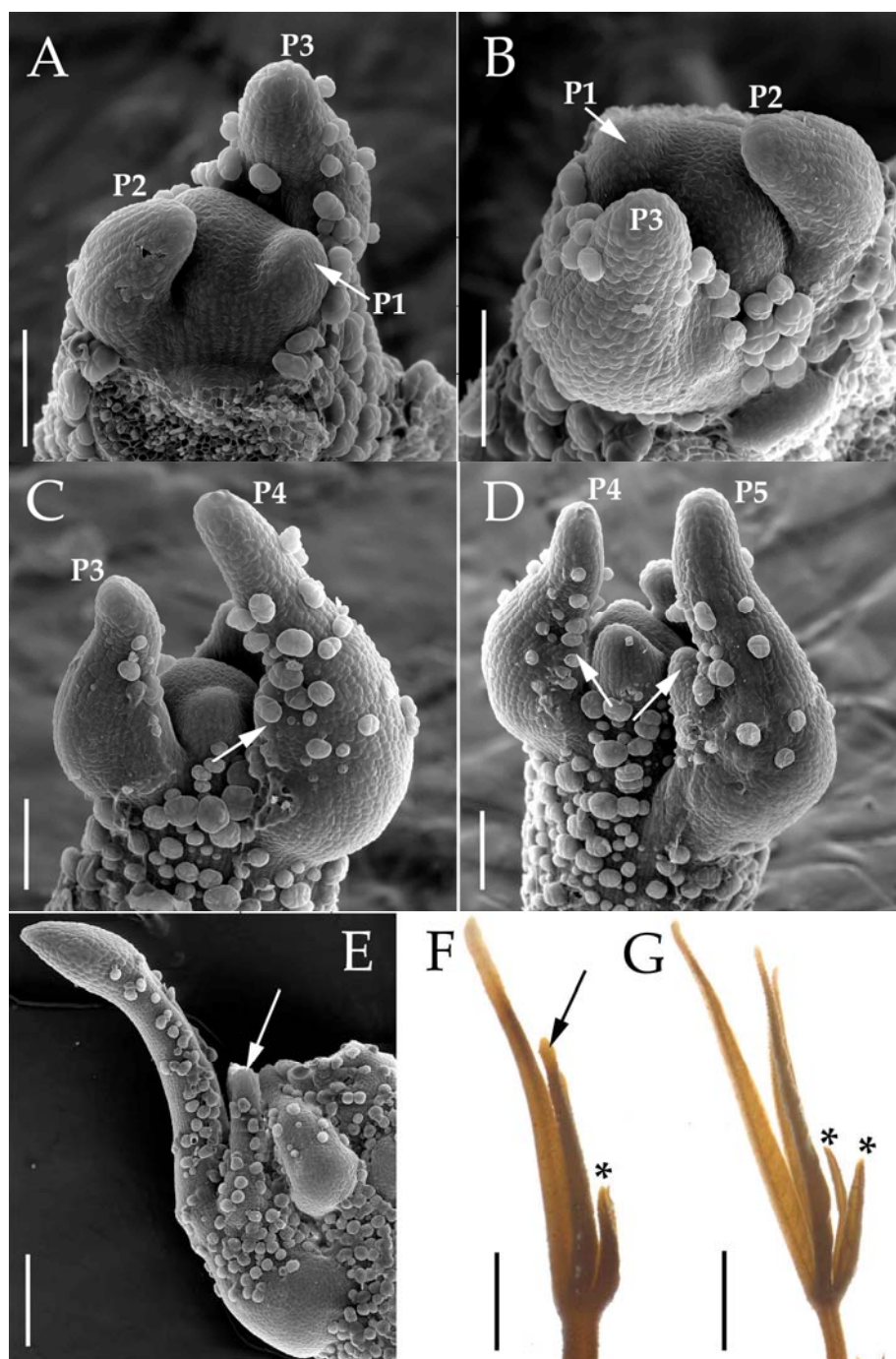


Figure 6. Leaf Development in *I. cairica*. (A-E) SEM images depicting early stages in leaf development. (A-B) P1-P4 stages. (C-E) Later primordium stages (P3~P6) showing the development of the first pair of lateral lobes. (F-G) Young leaves showing blade expansion and elongating lateral lobe pairs. Scale Bars: (A-D) 100µm. (E) 250µm. (F) 1mm. (G) 2mm. First marginal lateral lobes (arrows). Proximal lateral lobes (asterisks).

distinguishable (Fig 6A-B). Also at this stage, trichomes rapidly appear on both the adaxial and abaxial side of the primordium (Fig 6A). Marginal expansion continues and a protrusion begins to form, soon after recognizable as lateral lobes (Fig 6C-D, arrows). These lateral lobes become easily distinguishable from the terminal lobe (Fig 6D-F, arrows). Two additional lobes are initiated later in development proximally to the original pair, and will remain smaller in size than the first-formed lateral lobe pair (Fig 6F-G, asterisks). All parts of the young leaf remain folded until relatively late in development (leaf is ~8mm) (Fig 6G) and unfold when approaching maturity (Fig 1D).

### Vein Homology

The comparison of developmental leaf morphology between species revealed commonalities. Namely, all species exhibited an initial elongation of the primordium and development of the distal identity of the leaf, followed by morphological changes along the proximal blade region. This proximal region corresponds to the broadening of the cordate base in *I. purpurea* and *I. coccinea*, the separation of the leaf margin into deep or filamentous lobes in *I. sloteri* and *I. quamoclit*, respectively, and complete separations of the blade into leaflets in *I. cairica* (Fig 1A-E). The mature morphology of each species shows that the proximal blade regions correspond to the two major vascular strand pairs that

split at the petiole-blade junction in all species. In the interest of conducting a morphometric analysis, the homology of these vein pairs was investigated developmentally and anatomically. The investigation was based on the spatial relation of differentiating xylem (tracheary elements) of the vein pairs to the common petiolar vascular arrangement in which a central vascular arc (CA) is separated from two distinct adaxial bundles (Ad). Since the procambial vein pattern is predetermined and set in very young leaf primordia, prior to the tracheary element differentiation, and the fact that a visible marker of procambium is unavailable in *Ipomoea*, tracheary element differentiation (as indicated by lignin deposition) was observed through dark field illumination to view vascular strands. Differentiation of xylary elements follows that of the procambial pattern and is therefore a reliable visual marker of the vein pattern in young developing leaves (Kang and Dengler 2004). Figures 7-11 show cleared young leaves highlighting xylem strand differentiation through the petiole and into the blade, as well as a mature petiole transverse section showing the arrangement of vascular bundles.

### *I. purpurea*

Vascular strand differentiation begins with the midvein (MV) as the primordium emerges and elongates from the SAM flank (Fig 7A). As blade

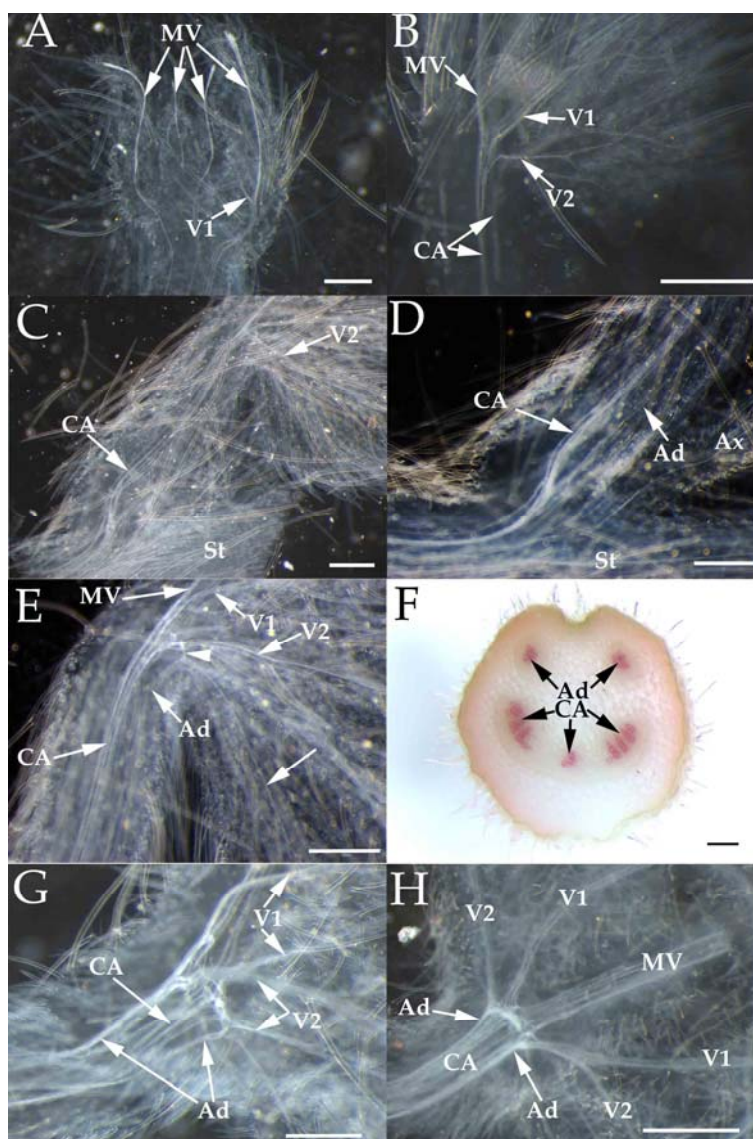


Figure 7. Vascular Strand Differentiation in *I. purpurea*. (A-E) Chloral-hydrate clearings of intermediate leaf stages showing vascular differentiation. (A) Young leaves surrounding the apex. (B) Young leaf with differentiating V1 and V2 veins. (C) Petiole of young leaf with branching of central arc from the stem visible, no visible adaxial bundles. (D) Petiole base with adaxial bundles visible. (E) Same leaf as in (D), with adaxial bundle supplying petiole-blade junction and a minor marginal vein. (F) Petiole transverse section stained with phloroglucinol. (G-H) Petiole-blade junction regions of mature leaves, cleared with chloral hydrate. Adaxial bundles can be traced into V2, while central arc bundles can be traced into V1. Scale Bars: (A-D,E,G) 500 $\mu$ m (F) 200 $\mu$ m (H) 1mm. Marginal minor vein (arrow). Branch from adaxial bundle (arrowhead).

expansion progresses, the two pairs of major veins become visible as xylem differentiation begins at the petiole-blade junction and progresses into the blade. The first pair to begin differentiation lies distally within the blade (V1), relative to the next pair to differentiate (V2) (Fig 7A-B). At this stage, multiple bundles of the central arc (CA) are also apparent (Fig 7B). As the petiole elongates and the blade continues to expand laterally, differentiation of the adaxial bundles in the petiole is not yet visible (Fig 7C). Shortly after this stage, the adaxial bundles become visible, differentiating acropetally within the petiole as these strands are first visible near the stem and differentiate progressively along the length of the petiole (Fig 7D), reaching the V2 vein pair that is already differentiating (Fig 7E, arrowhead), and also splitting into the proximal leaf margin (Fig 7E, arrow). As the leaf reaches full expansion, the arrangement of vascular bundles in the petiole is apparent, with two adaxial bundles completely spatially separate from the central arc (Fig 7F). In the mature leaf, tracing these vascular bundles through the petiole-blade junction and into the blade shows that the adaxial bundles lead into V2 veins through the petiole-blade junction and the central arc leads into V1 veins through the petiole-blade junction (Fig 7G-H).

*I. coccinea*

Vascular strand differentiation begins with the midvein (MV) (Fig 8A) with the central arc becoming apparent as adjacent strands progressively differentiate from near the stem into the petiole (Fig 8B). At this stage, differentiation of blade venation begins, V1 and V2 veins arise within the proximal region of the blade (Fig 8B). Differentiation for both vein pairs begins at the petiole-blade junction and progresses laterally into the blade (Fig 8B-C). The V1 veins differentiate first and will lie distally within the blade relative to corresponding V2 veins (Fig 8B-C). The adaxial petiole bundles also appear at this stage, differentiating first near the stem and progressing up the length of the petiole and into the V2 vein pair (Fig 8C-D). In the mature leaf, the vascular bundle arrangement in the petiole is apparent in transverse section (Fig 8F). As these vascular bundles are traced through the petiole and into the blade, it is apparent that the adaxial bundles lead into V2 veins through the petiole-blade junction and the central arc bundles lead into V1 veins through the petiole-blade junction (Fig 8G).

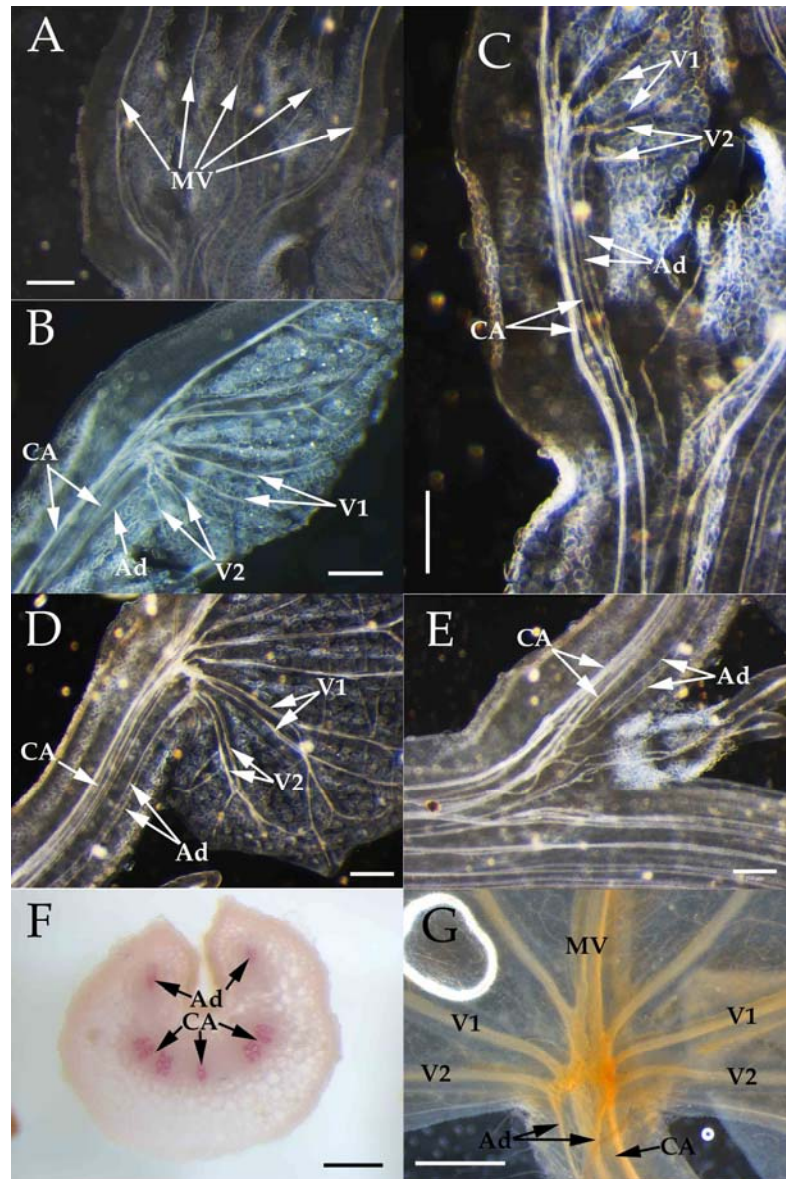


Figure 8. Vascular Strand Differentiation in *I. coccinea*. (A-E) Chloral-hydrate clearings of intermediate leaf stages showing vascular differentiation. (A) Young leaf stages surrounding the apex. (B) Young leaf with petiole adaxial bundles and major secondary vein pairs in the blade. (C) Young leaf with petiole adaxial bundles traceable from the petiole base through prospective V2 veins. (D) Intermediate leaf with V1 and V2 veins traceable to the central arc and adaxial bundles, respectively. (E) Petiole base from young leaf in (D) showing the divergence of the adaxial bundles from the central arc. (F) Transverse section of a mature petiole stained with phloroglucinol. (G) Petiole-blade junction of mature leaf cleared in chloral-hydrate. Scale Bars: (A-F) 200 $\mu$ m. (G) 1mm.

*I. sloteri*

Vascular differentiation begins acropetally with the midvein (MV) in young developing leaf primordia (Fig 9A). Shortly thereafter, the marginal lobes begin to develop laterally and secondary veins begin to differentiate basipetally down the leaf primordia (Fig 9A, arrowheads). The most proximal of these veins, and therefore the last to differentiate, are the V1 and V2 vein pairs, with differentiation for both beginning at the petiole-blade junction and progressing laterally towards the leaf margin (Fig 9B). Concurrently, adaxial bundles begin to differentiate acropetally through the petiole (Fig 9B-D), and along the prospective V2 veins (Fig 9C,E). At maturity, the adaxial bundles and the central arc are apparent in petiole transverse section (Fig 9F). As these bundles are traced into the blade through the petiole-blade junction, it is apparent that adaxial bundles lead into V2 veins through the petiole-blade junction, and that central arc bundles lead into V1 veins through the petiole-blade junction (Fig 9G).

*I. quamoclit*

Vascular strand differentiation begins with the midvein (MV) after considerable proximal-distal elongation of the primordium (Fig 10A). Simultaneous with midvein differentiation is the basipetal initiation of marginal lobes

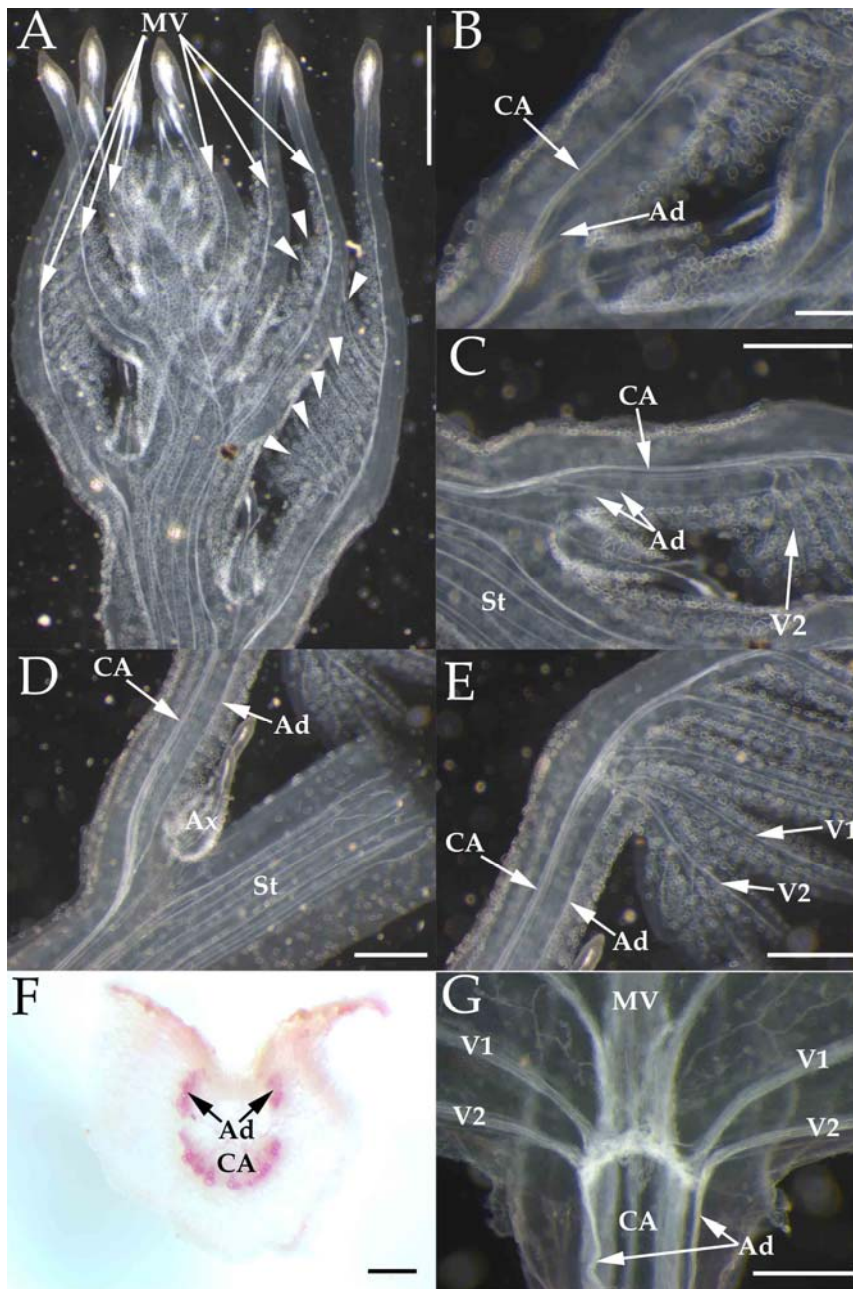


Figure 9. Vascular Strand Differentiation in *I. sloteri*. (A-E) Chloral-hydrate cleared young leaf stages showing vascular differentiation. (A) Young leaf primordia surrounding the apex. (B-C) Young leaf petiole showing adaxial bundle differentiation. (D) Petiole base showing spatial separation of adaxial bundles from central arc. (E) Petiole-blade junction near maturity showing relation between petiole and blade vasculature. (F) Mature petiole transverse section stained with phloroglucinol. (G) Petiole-blade junction of mature leaf cleared in chloral-hydrate. Scale Bars: (A) 1mm. (B,F) 200 $\mu$ m. (C-D,F) 500 $\mu$ m.

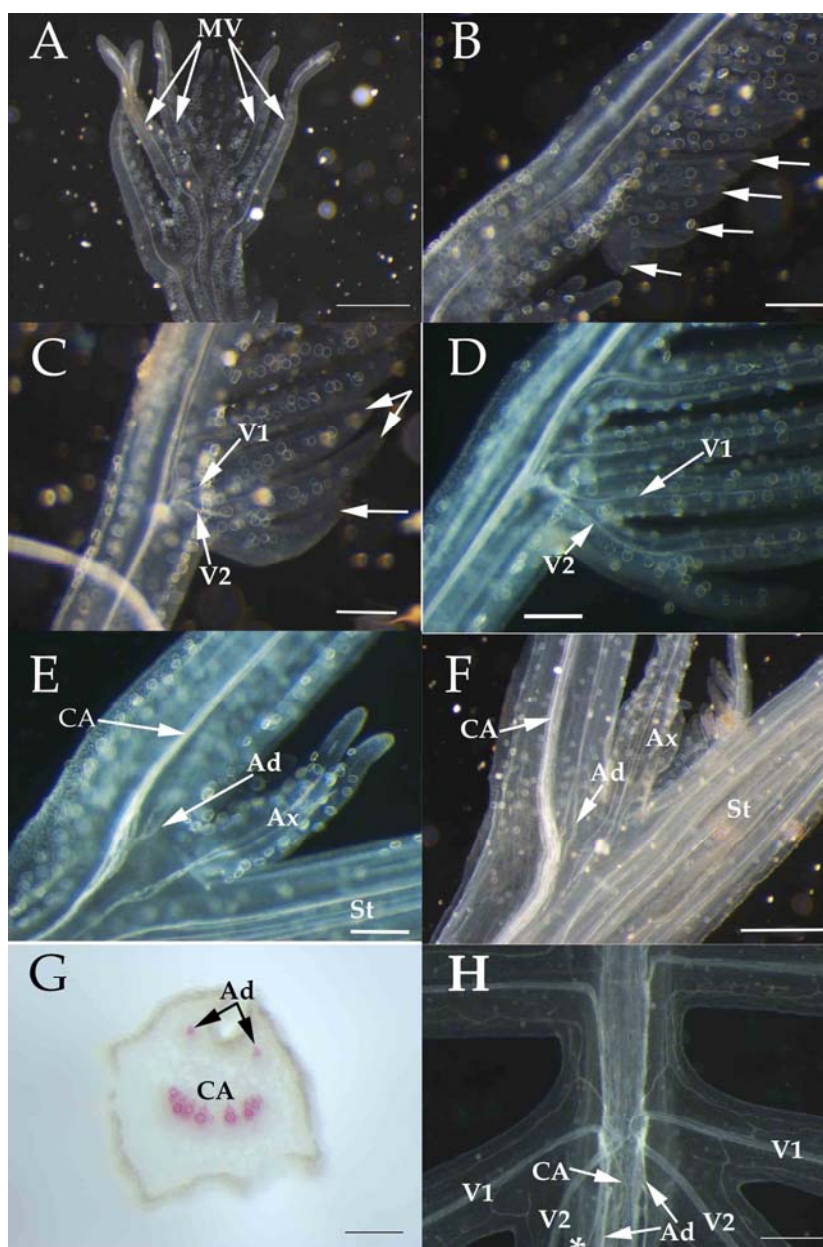


Figure 10. Vascular Strand Differentiation in *I. quamoclit*. (A-F) Chloral-hydrate cleared young leaf primordia showing vascular strand differentiation. (A) Young leaf primordia with differentiating midveins. (B) Marginal lobes elongate prior to secondary veins appearing. (C-D) Secondary veins differentiate in marginal lobes. (E-F) Differentiation of adaxial bundles along length of the petiole, (E) is petiole base of same leaf as in (D). (G) Mature petiole transverse section stained with phloroglucinol. (H) Petiole-blade junction of mature leaf cleared in chloral-hydrate. Scale Bars: (A,F,H) 500µm. (B-E,G) 200µm. Marginal lobes (arrows). Marginal vein (asterisk).

(Fig 10B, arrows). All lobes are initiated and have significantly elongated before major secondary veins within the lobes have differentiated (Fig 10B-C, arrows). These, including the two major pairs that arise from the petiole-blade junction (V1 and V2), differentiate along most of the length of the marginal lobes before adaxial bundles begin to differentiate in the petiole (Fig 10C-E). Adaxial bundles rapidly differentiate acropetally along the length of the petiole, and spatial separation of the adaxial bundles from the central arc is apparent near the petiole base (Fig 10F). At maturity, the arrangement of adaxial bundles and the central arc in the petiole is apparent in transverse section (Fig 10G). As these bundles are traced through the petiole-blade junction and into the blade, it is apparent that adaxial bundles lead into V2 veins through the petiole-blade junction, and that central arc bundles lead into V1 veins through the petiole-blade junction (Fig 10H). The adaxial bundles also contribute to minor veins that are present along the proximal margin of the most proximal lobe (V2 lobe) (Fig 10H, asterisk).

*I. cairica*

Vascular differentiation begins with the midvein (MV) in developing primordia (Fig 11A). Differentiation of major secondary vascular strands occurs

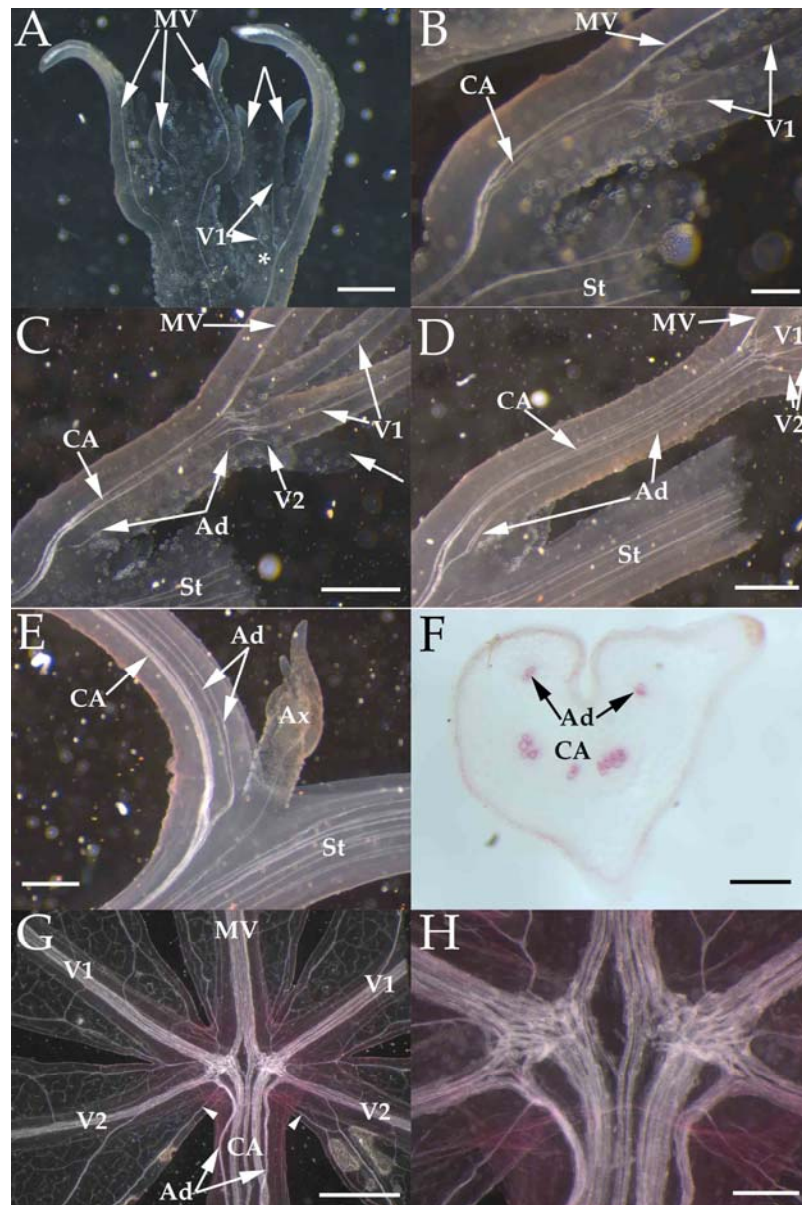


Figure 11. Vascular Strand Differentiation in *I. cairica*. (A-E) Chloral-hydrate cleared young stages showing vascular strand differentiation. (A) Young leaves surrounding apex with midveins. (B) V1 strand is continuous with petiole central arc. (C) Differentiation of petiole adaxial bundles and V2. (D) Continuity of adaxial bundles through length of petiole. (E) Spatial separation of adaxial bundles from central arc at the petiole base. (F) Mature petiole transverse section stained with phloroglucinol. (G) Petiole-blade junction of mature leaf cleared in chloral-hydrate. (H) High magnification of petiole-blade junction as shown in (G). Scale Bars: (A,C-E,H) 500 $\mu$ m. (B,F) 200 $\mu$ m. (G) 2mm. Vein discontinuity (asterisk). Marginal lobes (arrows). Marginal minor veins (arrowheads).

after considerable elongation of the first and most distal pair of marginal lobes (Fig 11A, arrows). These secondary veins differentiate discontinuously with the midvein and petiole vasculature (Fig 11A, asterisk), but reconnect at the petiole-blade junction and into the central arc (Fig 11A-B). As this distal marginal lobe pair, containing the V1 veins, continues to elongate, the proximal lobes expand laterally (Fig 11C, arrow). Simultaneously, the adaxial bundles of the petiole and V2 veins differentiate along the length of the petiole and into the proximal lobes (Fig 11C). As the leaf nears maturity, the differentiation of the adaxial bundles becomes continuous along the length of the petiole (Fig 11D), and is spatially separated from the central arc near the petiole base (Fig 11E). In the mature leaf, this arrangement of petiole vasculature is apparent in transverse section (Fig 11F). By tracing these bundles as they differentiate, it is apparent that adaxial bundles lead into V2 veins through the petiole-blade junction, and that central arc bundles lead into V1 veins through the petiole-blade junction (Fig 11G-H). The adaxial bundles also branch into a pair of minor veins that run along the margins of the most proximal leaf lobe (Fig 11G, arrowheads).

### Common Vein Pattern

Despite the notable differences in mature leaf shape between species, a common pattern of major vascular strand differentiation in the petiole and blade is apparent. The pattern of differentiation can be followed as V1 and V2 vein pairs differentiate laterally into the blade from the petiole-blade junction, where central arc bundles lead into the midvein, while adaxial bundles in the petiole differentiate acropetally from the petiole base through to the blade and become continuous with V2 vascular strands. The arrangement of vascular bundles in the mature leaf is common across the five species and can be traced from the stem, through the petiole and into the leaf blade. It begins with the divergence of the leaf vascular trace from that of the stem vascular bundles and the axillary (Ax) bud (see Fig 11E). Shortly thereafter, two bundles from the central arc diverge adaxially and remain spatially separated into the two adaxial bundles and the central arc, respectively (see Fig 11E). All vascular bundles of the petiole vasculature contribute to a collection of strands at the petiole-blade junction. Additionally, the outer strands of the central arc continue into the blade and form one of the major secondary vein pairs, the V1 veins. The petiole adaxial bundles also continue to differentiate towards the leaf blade and form the second major secondary vein pair, the V2 veins. This pattern is consistent across species

despite the drastic differences in the blade morphology (Fig 7-11), supporting that two major vein pairs that diverge from the petiole-blade junction are homologous across species.

### Morphological Analysis

Given the support shown for the homology of proximal vein pairs in the five *Ipomoea* species, a morphometric analysis was performed on mature leaf samples from each. Six landmarks were assigned along the leaf margin corresponding to the trajectories of the homologous major veins (Fig 12). These

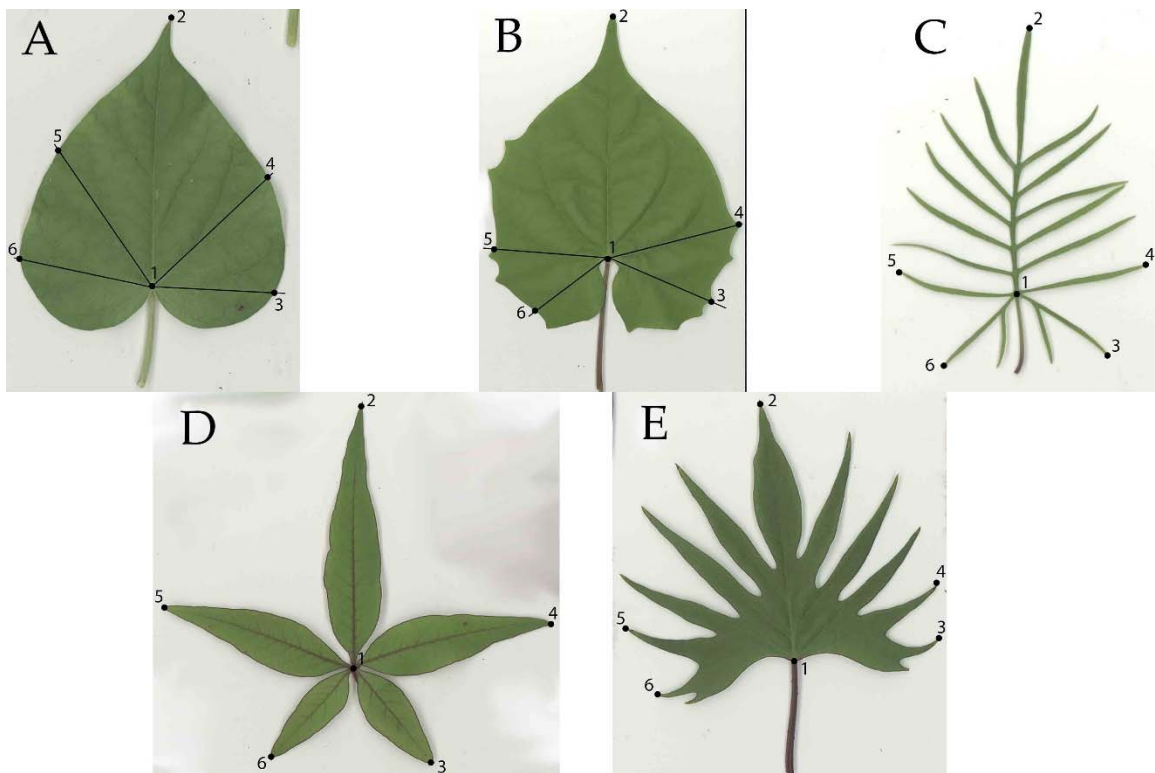


Figure 12. Procrustes Landmarks Plotted on Mature Leaves of Each Species. (A) *I. purpurea*. (B) *I. coccinea*. (C) *I. quamoclit*. (D) *I. cairica*. (E) *I. sloteri*.

landmarks represent the midvein and the two major secondary vein pairs (V1 and V2) arising from the petiole-blade junction. In the species with lobed or dissected leaves, *I. sloteri*, *I. quamoclit*, and *I. cairica*, these major veins all terminate at the blade margin and thus, landmarks were assigned to these points (Fig 12 C-E). In the simple-leafed species, *I. purpurea* and *I. coccinea*, major secondary veins form loops with adjacent vascular strands, thus terminating at points that are neither representative of the original vein trajectory or consistent with the landmarks assigned to lobed and dissected species. For this reason, landmarks in simple species corresponding to major secondary veins were established by extending the initial trajectory of the vein from the petiole-blade junction through to the margin (Fig 12A-B).

These six landmarks were plotted onto digital images of mature leaves of each species. A generalized procrustes analysis was performed on the data set, effectively removing differences in size and rotation between samples. Scaled and rotated data point sets were plotted for each species, along with density contours to aid in the visualization of point clusters (Fig 13). Twelve principal components (PCs) describe the shape variation among the six landmarks used. Of these, the first six account for 97.8% of the total. Species shape variances are represented along each of these PCs in tangent morphospace, in which each

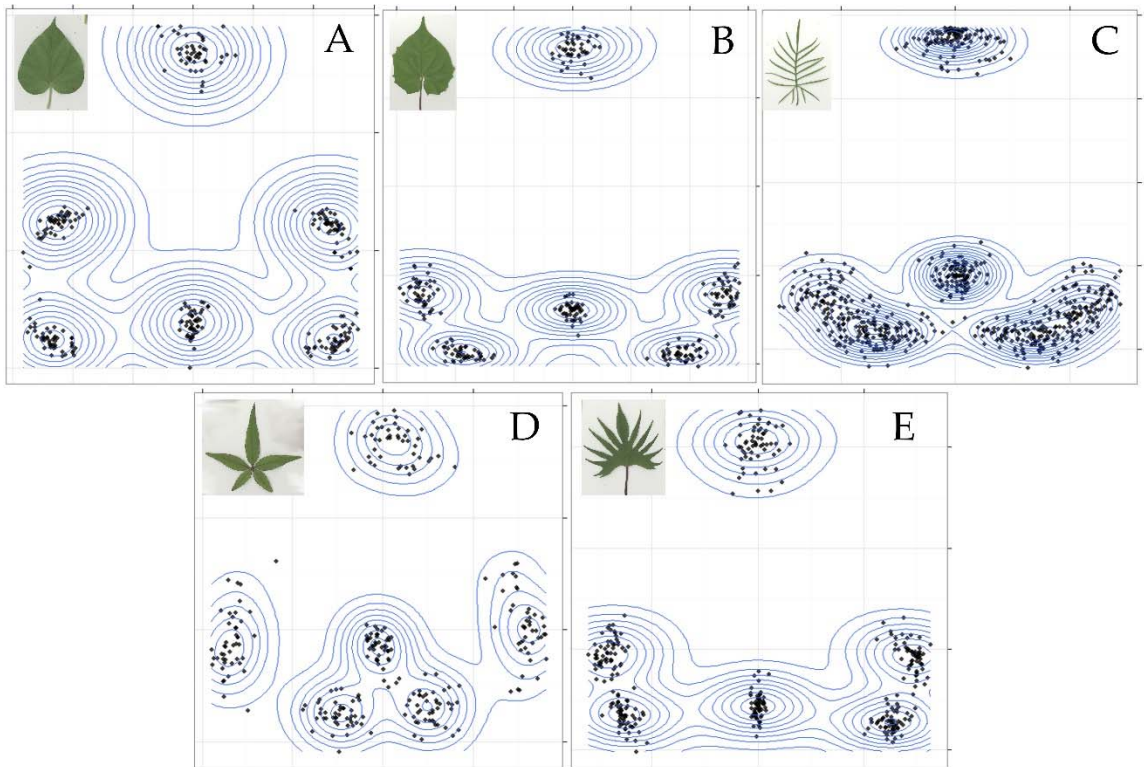


Figure 13. Species Landmarks After Scaling and Rotation. (A) *I. pupurea*. (B) *I. coccinea*. (C) *I. quamoclit*. (D) *I. cairica*. (E) *I. sloteri*.

point represents the six-landmark shape of an individual leaf sample (Fig 14-19). Pairwise t-tests were performed so that the mean of every species was compared to the mean of every other statistically for each PC. In this way, statistical significance of the separation between species distribution means can be tested along with a visualization of the distributions. Also shown for each PC are representative landmark shapes for the mean shape of all samples, and for extremes ( $\pm$  SD) on either side of the mean along the given PC.

The first PC accounts for 59.6% of the total variance, and therefore more than the rest of the PCs combined (Fig 14). Only *I. cairica* and *I. quamoclit* were shown to have significantly different means along PC1 by t-test ( $p < .05$ ), while the rest of the pairwise species comparisons fail to separate significantly (Table 1, Fig 14A). Much of this shape variation, appears to be characterized by shifts in landmarks 3, 4, 5, and 6 in relation to landmarks 1 and 2 (Fig 14B-D). The landmarks shift occurs proximally and laterally above the mean (Fig 14B), and distally and laterally below the mean (Fig 14D). This suggests that in the *I. cairica* and *I. quamoclit* leaves sampled, the two pairs of secondary veins in *I. cairica* tended to be rotated proximally about their common point of origin, the petiole-leaf junction, relative to their homologues in *I. quamoclit*. That no other paired means achieved significant separation also supports that much of the shape variation described by homologous major veins is conserved.

Further support for significant shape conservation is lent by the second PC, which accounts for 17.4% of the total shape variation (Fig 15). Along this PC, the distribution mean of *I. cairica* is significantly less than that of every other species (Table 2, Fig 15A), while none of the remaining four species means is significantly different from any other (Table 2). The shape variation described by this PC appears to be characterized mostly by medial-lateral shifts in landmarks

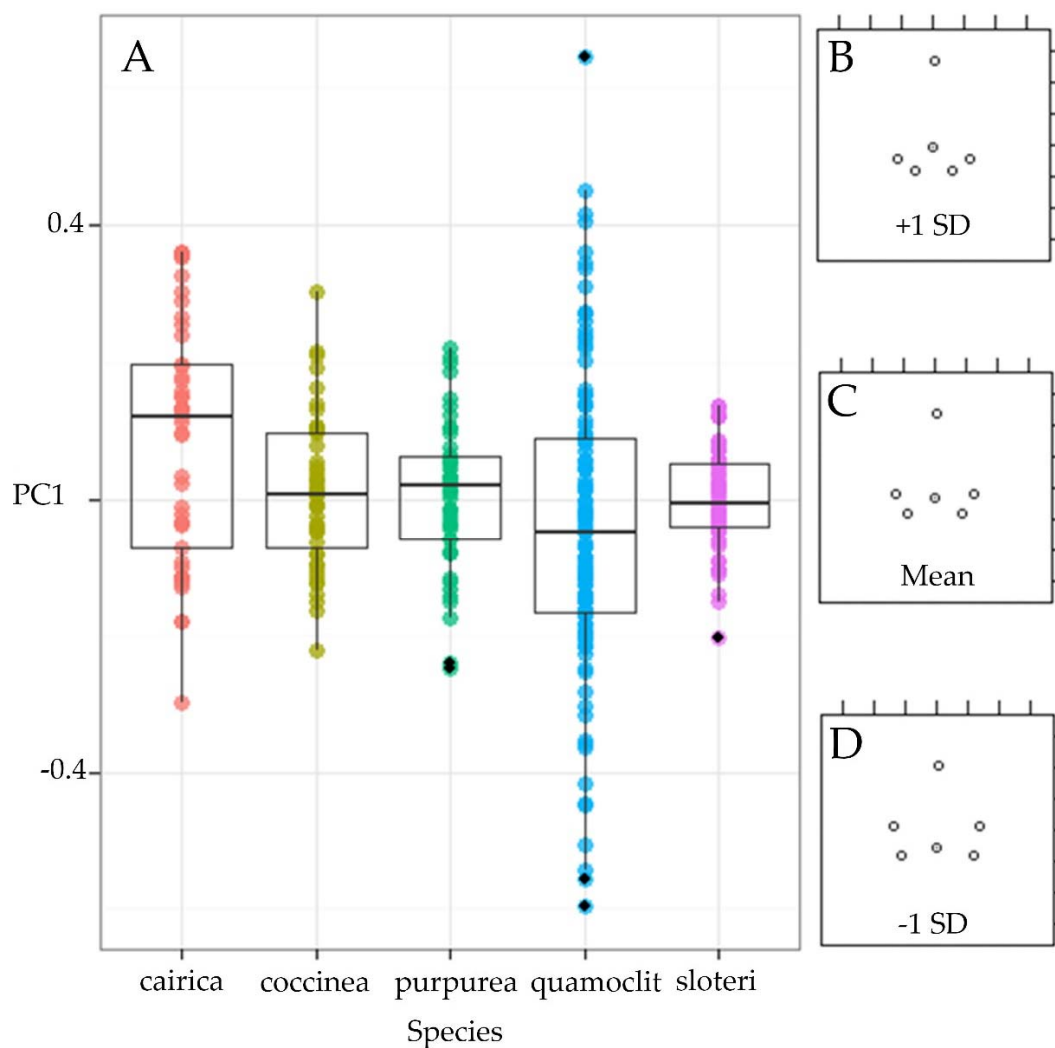


Figure 14. PC1 Describing 59.6% of Total Shape Variation (A) Distributions of tangent space values along PC1 for each species (B) Landmark shape at one standard deviation above the mean (C) The mean landmark shape (D) Landmark shape at one standard deviation below the mean

Table 1. P-values from Pairwise t-test of Means Along PC1. Significantly different distribution means are indicated by  $p < .05$  (asterisk)

	cairica	coccinea	purpurea	quamoclit
coccinea	.20393	-	-	-
purpurea	.16517	1.00000	-	-
quamoclit	.00017 *	.42820	.47527	-
sloteri	.06702	1.00000	1.00000	.55761

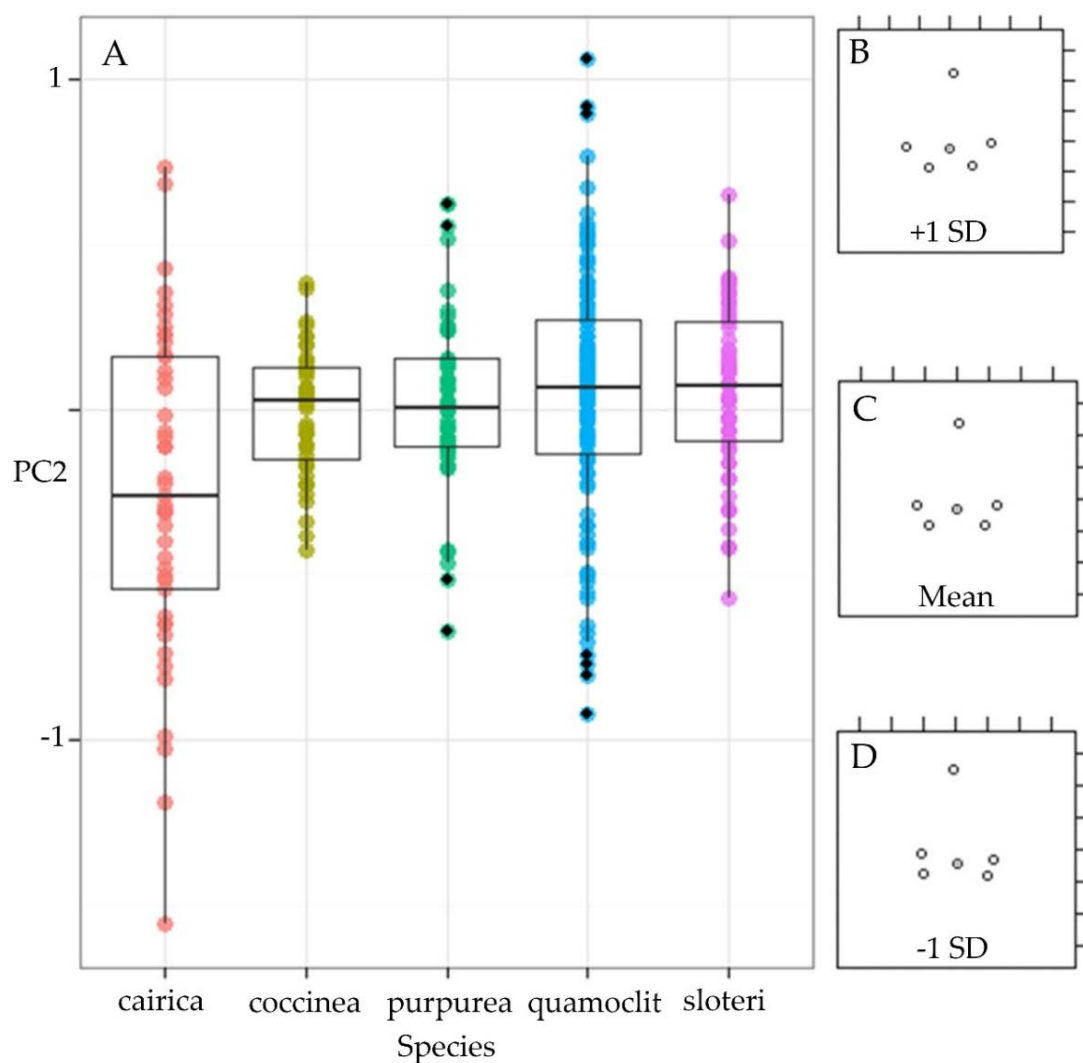


Figure 15. PC2 Describing 17.4% of the Total Variation (A) Distributions of tangent space values along PC2 for each species (B) Landmark shape at one standard deviation above the mean (C) The mean landmark shape (D) Landmark shape at one standard deviation below the mean

Table 2. P-values from Pairwise t-test of Means Along PC2. Significantly different distribution means are indicated by  $p < .05$  (asterisks)

	<i>cairica</i>	<i>coccinea</i>	<i>purpurea</i>	<i>quamoclit</i>
<i>coccinea</i>	.0064*	-	-	-
<i>purpurea</i>	.0016*	1.00000	-	-
<i>quamoclit</i>	1.2e-5*	1.00000	1.00000	-
<i>sloteri</i>	8.6e-5*	1.00000	1.00000	1.00000

3, 4, 5, and 6 relative to landmarks 1 and 2. Above the mean, landmarks 4 and 5 shift laterally, and landmarks 3 and 6 shift medially (Fig 15B). Below the mean, landmarks 4 and 5 shift medially and landmarks 3 and 6 shift laterally (Fig 15D). This would correspond to a leaf form in which the V1 veins elongate above the mean and shorten below the mean, relative to V2 veins. The data thus suggests that in the samples analyzed, the leaves of *I. cairica* tended to exhibit a ratio of V1 length to V2 length that was less than that of the rest of the species. The rest of the species pairs did not show significant separation along PC2. As this is also the case in PC1, combining the first two PCs shows that within the shape variation that describes 74.3% of the total, *I. purpurea*, *I. coccinea*, *I. quamoclit*, and *I. sloteri* show no significant separation from each other. This supports that much of the shape described by the homologous vein pattern between these species is conserved.

The shape variation described by PC3 accounts for 8.8% of the total (Fig 16). All species distribution means show significant separation from one another by t-test (Table 3, Fig 16A). The shape variation described by this PC includes left-right asymmetry that will be referred to here as handedness. This involves the landmarks on one side of landmark 1, being 3 and 4 to the right or 5 and 6 to the left, shifting distally while the opposite pair shifts proximally (Fig 16B-D).

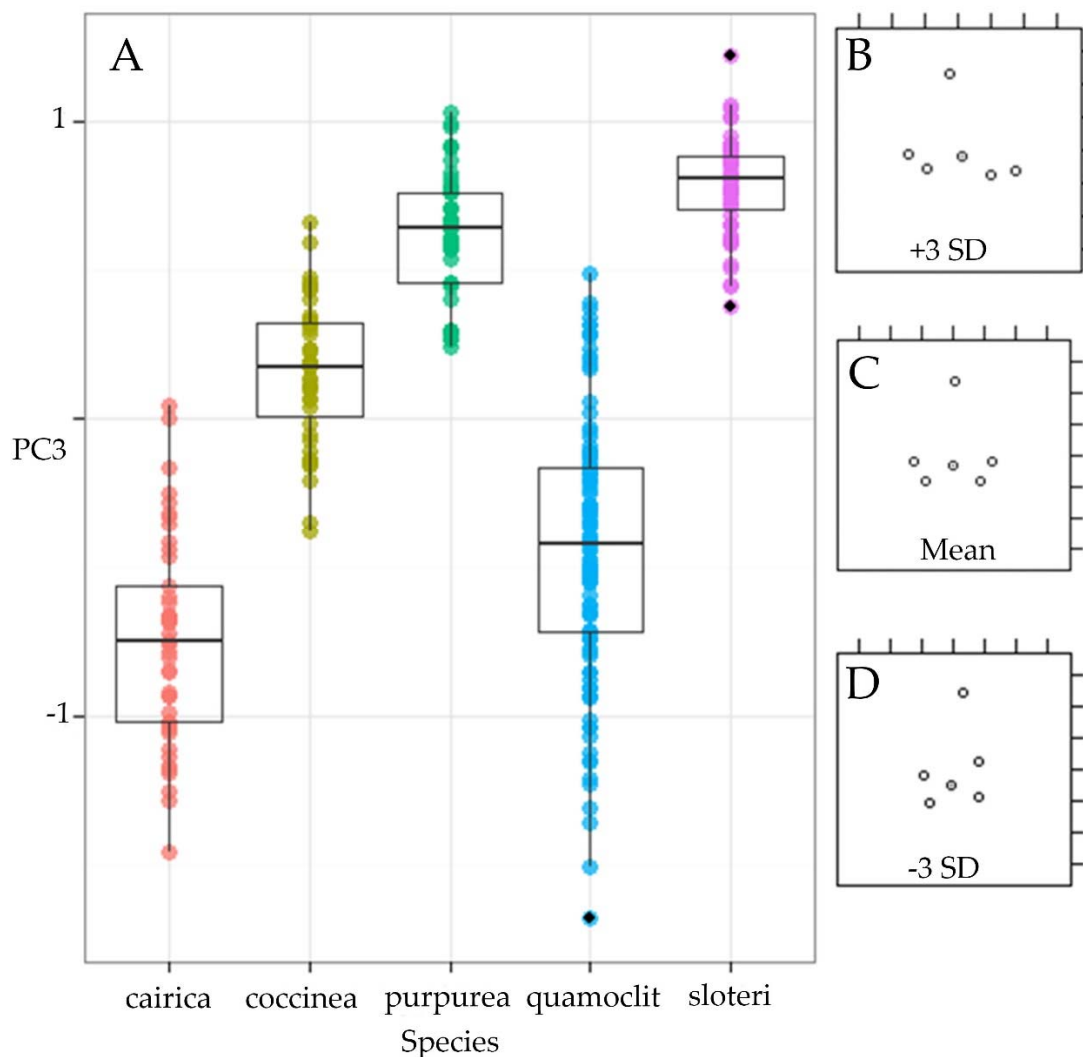


Figure 16. PC3 Describing 8.8% of the Total Variation (A) Distributions of tangent space values along PC2 for each species (B) Landmark shape at one standard deviation above the mean (C) The mean landmark shape (D) Landmark shape at one standard deviation below the mean

Table 3. P-values from Pairwise t-test of Means Along PC3. All differences in distribution means are significant ( $p < .05$ ).

	<i>cairica</i>	<i>coccinea</i>	<i>purpurea</i>	<i>quamoclit</i>
<i>coccinea</i>	< 2e-16	-	-	-
<i>purpurea</i>	< 2e-16	1.0e-10	-	-
<i>quamoclit</i>	2.9e-7	< 2e-16	< 2e-16	-
<i>sloteri</i>	< 2e-16	< 2e-16	.0081	< 2e-16

Additionally, landmark 2 shifts left or right of the mean toward the distally shifted pair (Fig 16B-D). This side is the side of handedness. The shift above the mean along PC3 is towards a left-handed configuration (Fig 16B), while the shift below the mean is towards a right handed configuration (Fig 16D).

Simultaneous with shifts in handedness, changes occur in the positions of landmarks 3 and 4 on the right, and 5 and 6 on the left relative to each other.

Above the mean, landmarks 4 and 5 shift laterally and proximally relative to landmarks 3 and 6, respectively (Fig 16B). Below the mean, landmarks 4 and 5 shift medially and distally relative to landmarks 3 and 6 respectively (Fig 16D).

These shifts correspond to leaf shapes in which, above the mean as in *I. purpurea* and *I. sloteri* (Fig 16A), V1 veins are longer relative to V2 veins, V1 and V2 veins are in closer proximity, and the leaf exhibits left-handedness. Below the mean as in *I. cairica* and *I. quamoclit* (Fig 16A), the shifts correspond to leaf shapes in which V1 and V2 veins are closer in length but more separate in space, and the leaf exhibits right-handedness.

The shape variation described by PC4 accounts for 8.4% of the total (Fig 17). All species distribution means show significant separation from one another by t-test (Table 4, Fig 17A). Again, shape variation is characterized in part along this PC by shifts in handedness. Landmark shifts are right-handed above the

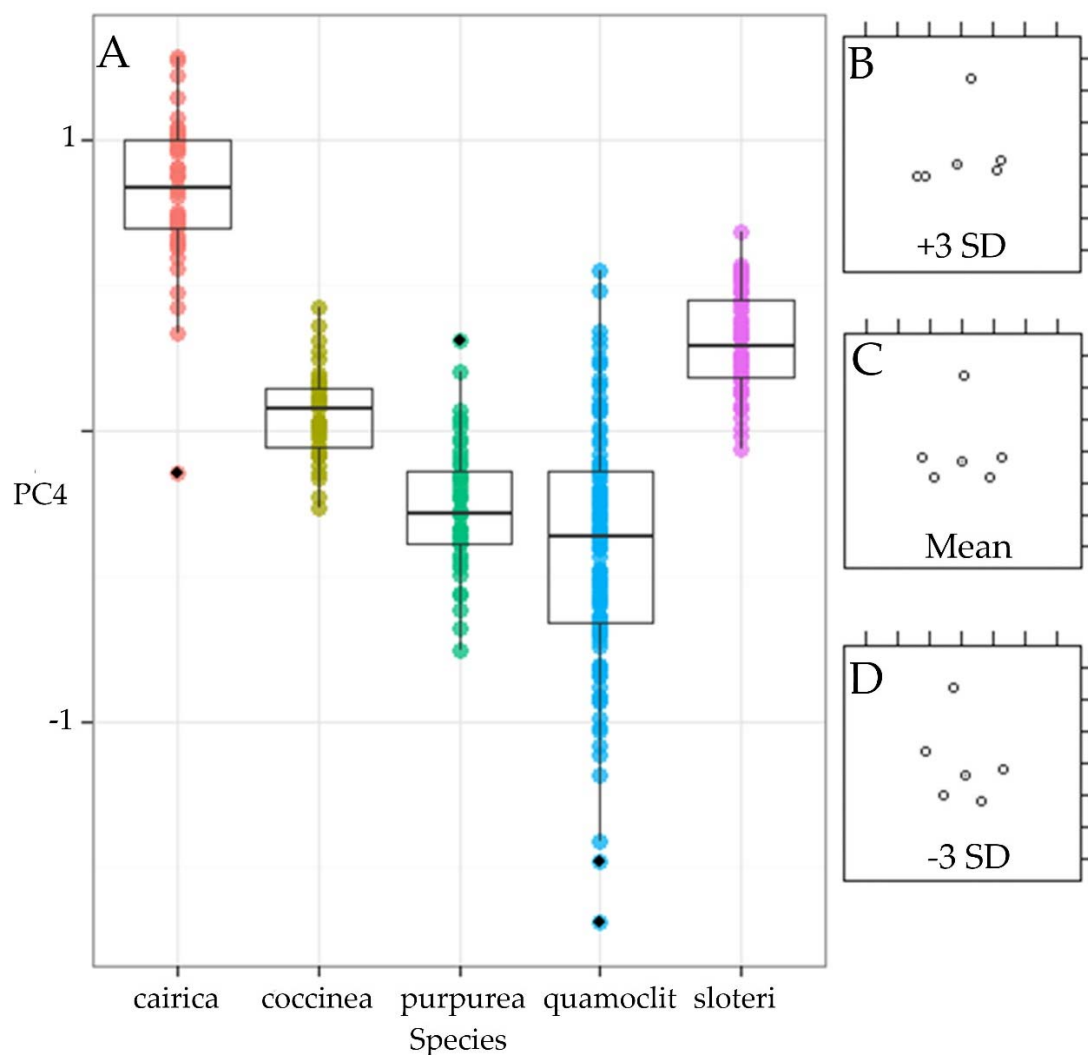


Figure 17. PC4 Describing 8.4% of the Total Variation (A) Distributions of tangent space values along PC2 for each species (B) Landmark shape at one standard deviation above the mean (C) The mean landmark shape (D) Landmark shape at one standard deviation below the mean

Table 4. P-values from Pairwise t-test of Means Along PC4. All differences in distribution means are significant ( $p < .05$ ).

	<i>cairica</i>	<i>coccinea</i>	<i>purpurea</i>	<i>quamoclit</i>
<i>coccinea</i>	< 2e-16	-	-	-
<i>purpurea</i>	< 2e-16	9.5e-7	-	-
<i>quamoclit</i>	< 2e-16	< 2e-16	.0059	-
<i>sloteri</i>	6.2e-16	4.4e-5	< 2e-16	< 2e-16

mean (Fig 17B) and left handed below the mean (Fig 17D). Additionally, above the mean, landmarks 4 and 5 approach landmarks 3 and 6, respectively (Fig 17B). Below the mean, the same respective landmarks separate from each other (Fig 17D). These shifts correspond to leaf shapes in which, above the mean as in *I. cairica* and *I. sloteri* (Fig 17A), V1 and V2 veins are in closer proximity and the leaf exhibits right-handedness. Below the mean, as in *I. quamoclit* and *I. purpurea* (Fig 17A), the shifts correspond to leaf shapes in which V1 and V2 veins are more separated spatially and the leaf exhibits left-handedness.

The shape variation described by PC5 accounts for 3.6% of the total (Fig 18). All species distribution means show significant separation from one another by t-test (Table 5, Fig 18A). Shape variation along this PC appears to be characterized above the mean by the collapse of all other landmarks toward landmark 1, accompanied by very slight left-handedness (Fig 18B). Below the mean, variation is characterized by the expansion of all other landmarks away from landmark 1, accompanied by very slight right-handedness (Fig 18D). The landmark shifts appear to correspond to leaf shapes in which the V2 veins and midvein shorten above the mean, as in *I. quamoclit* (Fig 18A) and lengthen below the mean, as in *I. cairica* and *I. sloteri* (Fig 18A), as the largest shifts appear to occur in landmarks 2, 3, and 6.

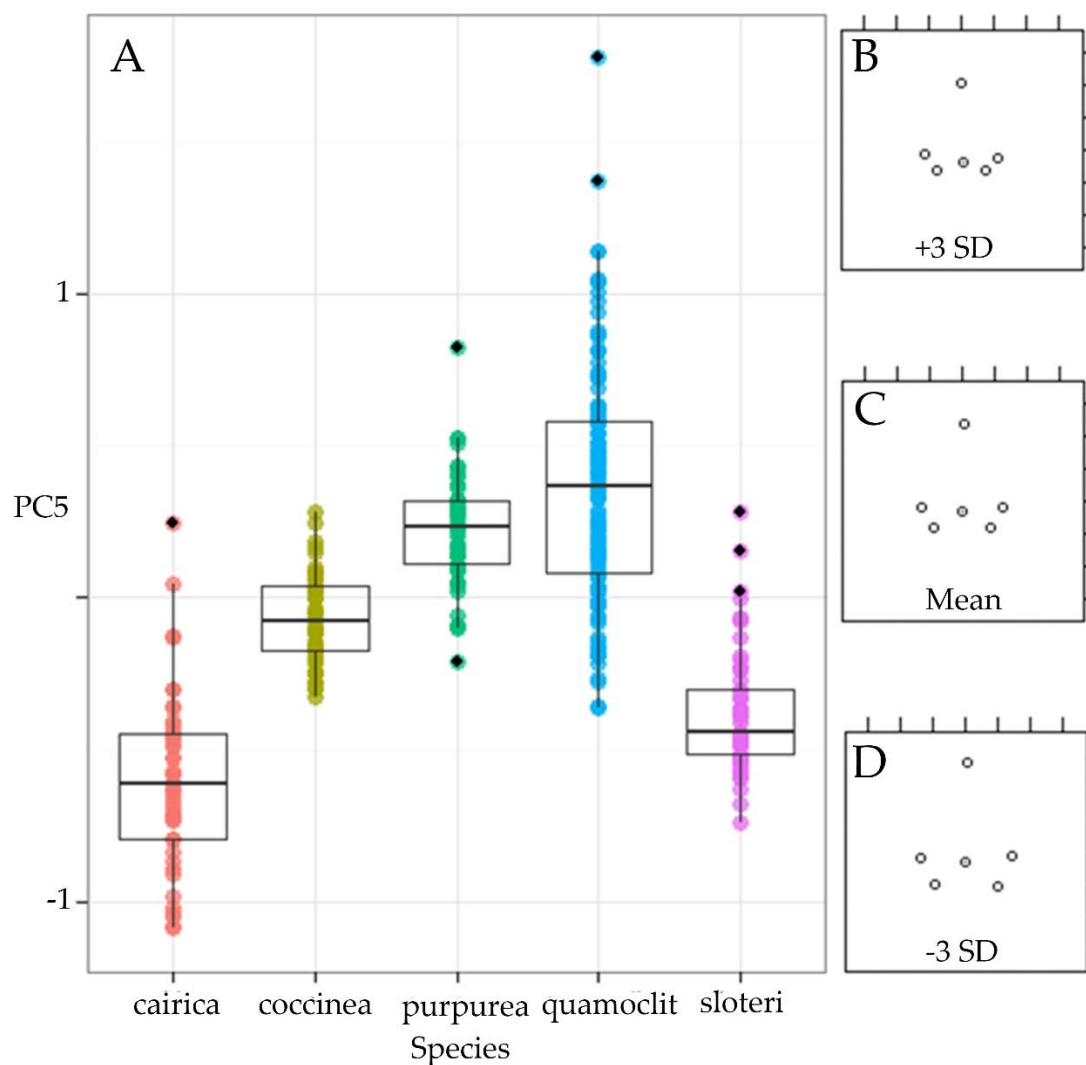


Figure 18. PC5 Describing 3.6% of the Total Variation (A) Distributions of tangent space values along PC2 for each species (B) Landmark shape at one standard deviation above the mean (C) The mean landmark shape (D) Landmark shape at one standard deviation below the mean

Table 5. P-values from Pairwise t-test of Means Along PC5. All differences in distribution means are significant ( $p < .05$ ).

	<i>cairica</i>	<i>coccinea</i>	<i>purpurea</i>	<i>quamoclit</i>
<i>coccinea</i>	3.8e-16	-	-	-
<i>purpurea</i>	< 2e-16	5.2e-6	-	-
<i>quamoclit</i>	< 2e-16	1.4e-15	.00389	-
<i>sloteri</i>	.00019	4.1e-7	< 2e-16	< 2e-16

The shape variation described by PC6 accounts for 2.7% of the total (Fig 19). All species distribution means show significant separation from one another by t-test (Table 6, Fig 19A). Shape variation along this PC appears to be characterized by the simultaneous approach and separation of left and right landmark pairs (Fig 19B-D). Above the mean, landmarks 5 and 6 approach each other while landmarks 3 and 4 separate (Fig 19B), while below the mean, landmarks 3 and 4 approach each other while landmarks 5 and 6 separate (Fig 19D). These shifts correspond to a leaf shape above the mean, as in *I. cairica* and *I. quamoclit* (Fig 19A), in which the V1 vein and V2 vein on the left side are in close proximity and those on the right side are separate. The opposite is true below the mean, as in *I. purpurea* and *I. sloteri* (Fig 19A), with the right V1 vein and V2 vein in close proximity and those on the left separate.

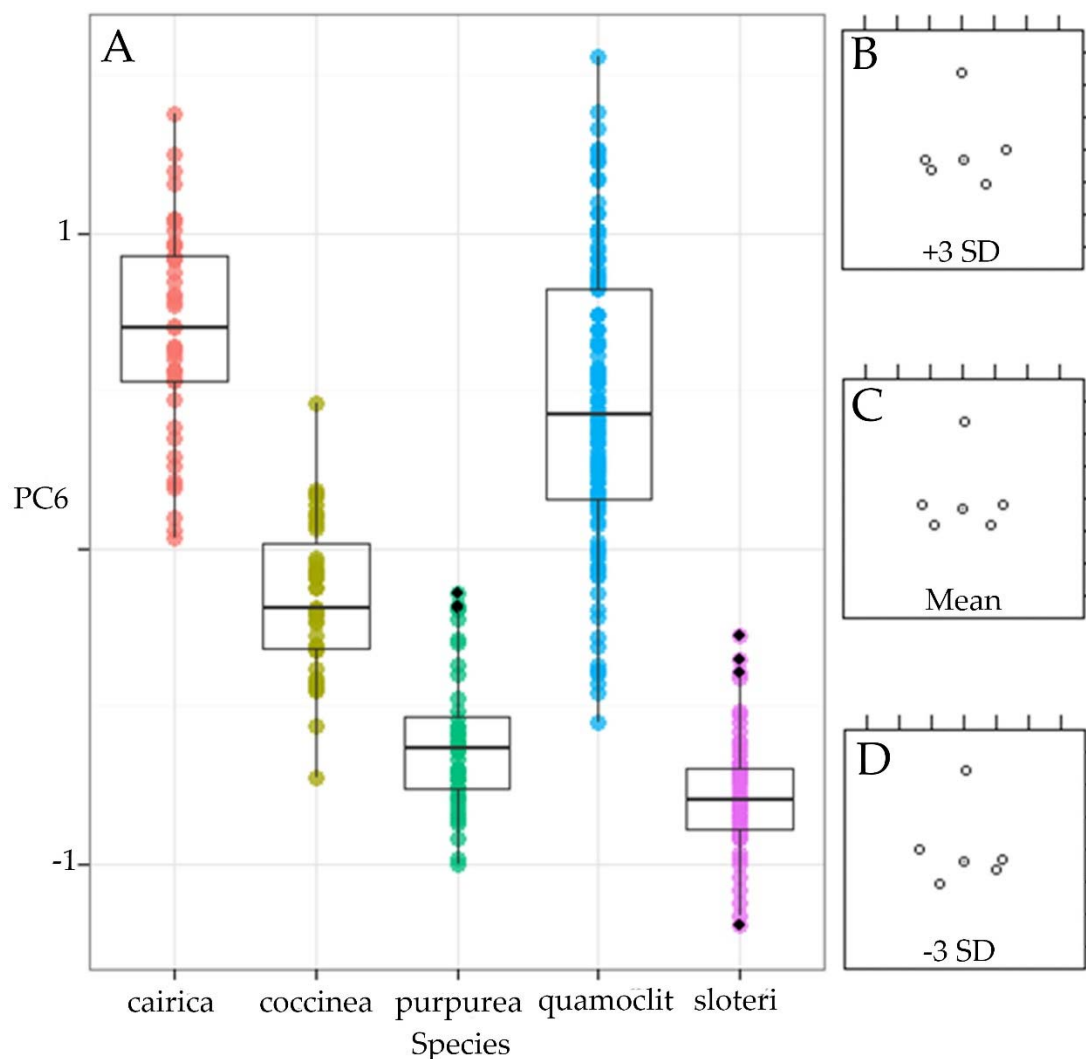


Figure 19. PC6 Describing 2.7% of the Total Variation (A) Distributions of tangent space values along PC2 for each species (B) Landmark shape at one standard deviation above the mean (C) The mean landmark shape (D) Landmark shape at one standard deviation below the mean

Table 6. P-values from Pairwise t-test of Means Along PC6. All differences in distribution means are significant ( $p < .05$ ).

	cairica	coccinea	purpurea	quamoclit
coccinea	< 2e-16	-	-	-
purpurea	< 2e-16	6.9e-10	-	-
quamoclit	.0003	< 2e-16	< 2e-16	-
sloteri	< 2e-16	< 2e-16	.0117	< 2e-16

## CHAPTER 4

## DISCUSSION

The analysis of external morphology of the leaf from initiation through to maturity can aid significantly in the analysis of mature leaf shapes. It has been shown that inherent patterns of vegetative development, including phyllotactic pattern, rate of leaf initiation, and clade-specific molecular action at initiation and shortly thereafter, can significantly impact the ultimate shape of the leaf (Bharathan et al. 2002; Chitwood, Headland, Ranjan, et al. 2012; Chitwood et al. 2007; Koenig et al. 2009; Scarpella et al. 2010). Therefore, understanding the developmental patterns by which leaves are initiated and subsequent growth that occurs within the young primordium can provide significant insights into the achievement of mature form. We find here that although a common spiral phyllotactic pattern and a similar early P1 morphology are shared across the five species, the differences in mature leaf form are reflected in young primordia.

Of particular interest here is the temporal initiation of marginal lobes and the appearance of trichomes, one of the traditional markers of cellular differentiation, on the leaf surface (Barth et al. 2009; Sylvester et al. 2001; Telfer et al. 1997). With this in mind the comparison of early primordium development in *I. coccinea*, *I. quamoclit*, and their hybrid *I. sloteri* provides an interesting example

when considering the assertion that dissected leaves spend more time in a transiently indeterminate state, allowing for the increase in marginal dissection (Barkoulas et al. 2008; Ben-Gera and Ori 2012; Ben-Gera et al. 2012; Berger et al. 2009; Champagne and Sinha 2004; Efroni et al. 2008; Kang and Sinha 2010; Ori et al. 2007; Shleizer-Burko et al. 2011; Vlad et al. 2014). The primordia of these three particular species exhibit a gradient in which the simplest leaf form, that of *I. coccinea*, develops the earliest, has the most dense trichome cover, and is the first to acquire a distinguishable margin along the length of the primordium (Fig 3). In comparison, the more dissected *I. sloteri* initiates trichomes less rapidly and is less densely covered, and initiation of the lobes along the length of the leaf margin is protracted (compared to *I. coccinea*) (Fig 4). Lastly, the primordia of the most dissected leaves, those of *I. quamoclit*, initiate the fewest trichomes and initiate the full complement of marginal lobes late into leaf development (Fig 5). Interestingly, the hybrid and intermediately dissected leaf form of *I. sloteri* also shows an intermediate rate of marginal lobe initiation and trichome density. These results support that more dissected forms within *Ipomoea* spend more time in a state of indeterminacy, as the primordia of *I. quamoclit* have the most protracted time to acquire the final mature form compared to *I. coccinea*, as well as showing less trichome density (Fig 5). The remaining members of this study,

*I. purpurea* and *I. cairica*, lend further support to this model, with the primordia of *I. purpurea* quickly developing extremely dense trichome cover as well as initiation of the leaf margin (Fig 2), while the primordia of *I. cairica* develop relatively sparse trichome cover and spend a longer time initiating the entirety of the five-lobed dissected margin (Fig 6).

Amidst the noticeably different patterns of growth across these species, commonalities are also identifiable, most notably the shared spiral phyllotactic pattern and the basipetal initiation of marginal outgrowths. This pattern of growth along the primordium margin is apparent in the lobed-leafed species *I. cairica*, *I. sloteri*, and *I. quamoclit*, as the most distal lobes are the first to arise and initiation proceeds successively in the proximal direction (Fig 4-6). Additionally, this process appears to be mimicked by the simple-leafed species, *I. purpurea* and *I. coccinea*, as the more extensive proximal growth which results in the cordate leaf base begins only after the margins have begun to expand (Fig 2-3).

The major molecular directors of vein pattern formation have been well established, consisting mostly, if not exclusively, of the response to PIN1-directed auxin transport (Koenig et al. 2009, Scarpella et al. 2010). Additionally, the HD-ZIP III gene and traditional procambium marker, AtHB8, although not directly needed for auxin response, has been shown to be necessary for

maintenance of cell files that lead to the vascular pattern amidst perturbations in directed auxin transport (Donner et al. 2010; Donner et al. 2009; Sawchuck et al. 2008; Scarpella et al. 2006; Scarpella et al. 2010). In most wild-type dicot leaves, all major vascular bundles in the leaf blade converge distal to or near the petiole junction, forming a singular leaf trace that extends through the petiole and into the stem (Roth-Nebelsick A 2001). The five present species of *Ipomoea* retain three separate traces, arranged in a similar pattern through most of the petiole length before convergence. This pattern, combined with the extreme likelihood of the described molecular determinants of vascular differentiation being active in these species, leads us to argue for the high probability that this leaf vascular pattern is the result of common ancestry, and can therefore be viewed as homologous across these species.

Givnish and Vermeij (1976) argue that leaves of understory liana plants tend to adopt a cordate leaf shape as a way of increasing leaf area per laminar unit, while supporting the development of erect petioles which may optimize the interception of filtered sunlight. The entire to three-lobed cordate shape is extremely frequent within *Ipomoea* (Appendix), suggesting that either this form arose early within the history of the clade and was subsequently lost in taxa like *I. quamoclit* due to laminar dissection, or that the shape arose many times across

the clade due to convergent evolution. The former seems more parsimonious given the frequency of the form within the genus, but as yet the history of leaf shape characters in *Ipomoea* has not been tested. Whatever the model for the evolutionary dynamics of leaf shape, evidence is shown here for a largely variable leaf blade construction around a highly conserved pattern of major vein differentiation. This supports the high degree of plasticity of elements of leaf shape amidst the strong conservation of other elements (Hasson et al. 2011; Jones et al. 2009; Piazza et al. 2010; Spinelli et al. 2011; Vlad et al. 2014). Tentatively, this would also support the role of HD-ZIP III genes like AtHB8, described above (Donner et al. 2010, Kang and Dengler 2004), as we observe a common vein pattern maintained amidst presumably divergent patterns of directed auxin transport.

The identification of the homology between vein patterns raised the question of whether the basic shape described by the vein trajectories was also conserved. The use of homologous points, represented by landmarks, in a morphometric analysis lends statistical rigor to analyses of shape variance, particularly when the interest is in removing size from consideration (Adams et al. 2004; Viscosi and Cardini 2011). The goal of the morphometric analysis performed here was to determine if clear differences in the arrangement of the

described homologous veins could be identified. Perhaps more interestingly, the majority of the species distribution means along most of the described shape variance (the first two PC's) failed to show significant differences (Fig 14-15). Moreover, along the rest of the described shape variation, all species distribution means did show significant separation (Fig 16-19). This provides an interesting basis on which to analyze the shape variation investigated here, but in order to do so, some points on interpreting morphometrics and this study in particular must be considered.

First, it is important to note that landmark distributions do not necessarily directly represent real-world shape changes. As all landmarks are free-floating in the shape space, all landmarks are to some degree affected by any localized change in shape (Viscosi and Cardini 2011). For example, if the only difference between two sample leaves was a difference in midvein length, namely a shift in the position of landmark 2 in the raw data, the analysis would distribute that shift amongst all six landmarks, rather than the one that reflects the actual natural variation. With many replicates, however, general trends representing major differences in shape should be reflected in the landmark distributions yielded from the procrustes analysis. Also, though the effect is likely minimal with regard to statistical analyses, distributions plotted in tangent shape space

are approximations of actual procrustes distributions. This is due to the procrustes shape space being hemispherical and data points, in order to be more easily interpreted, being projected orthogonally from this space to a two-dimensional plane tangent to the point representing the mean shape value (Slice 2001). Despite these two removals from real natural variation, these methods using landmarks or other shape descriptors have been proven effective in determining significant changes in shape (Chitwood et al. 2014; Chitwood, Headland, Ranjan, et al. 2012; Perez-Perez et al. 2011; Viscosi and Cardini 2011).

Likely more important to consider when interpreting morphometric results here are some inherent drawbacks in the experimental design. Among distinct species such as these, it is possible that significant differences exist in life history variables like growth rate and maturation rate. This being the case, since leaf number collected and growth conditions were kept constant, it is possible that the leaves collected across species represent different physiological stages, which could manifest themselves morphologically. This was compensated for by not using a pre-set time interval for growth before harvest, but rather collecting only after respective fifth leaves were deemed to have reached maturity. This potentially avoids much of the error due to differences in growth rate and environmental preferences, but also leaves room for error in that harvest time is

arbitrary and at the discretion of the collector. We operate under the assumption here that the mature shapes of all leaves were established at the time of collection, and that under the conditions used, no species were physiologically altered outside their natural range in a way that would significantly alter leaf shape. It should be kept in mind, however, that these factors combined with uncontrollable variables like very slight differences in light, water, or soil amount and quality, could create a degree of statistical noise causing increases in variances or decreases in precision along the considered PC's.

Of the most interest here is that most of the species leaf shape means failed to separate along the first two PC's, describing the majority of shape variation (Fig 14-15). The only significant differences that occurred were concerning *I. cairica*, a highly lobed leaf form in which the major veins considered are essentially free from one another. The other four species failed to separate from one another over this described 74.3% of the total shape variation. This indicates that the lengths and orientations of the major veins analyzed here are relatively conserved across these species despite extreme variation in the leaf form defined by the lamina. Also, from what is seen in the representative landmark shapes, recognizable and relatively isolated landmark shifts are seen along both of these PC's. Also indicated is that the conserved shape is not

necessarily well-defined and static, but rather that among individuals (48 for *I. purpurea*, 46 for *I. coccinea*, 59 for *I. sloteri*, 113 for *I. quamoclit*, and 45 for *I. cairica*), most of the species show very similar shifts in vein shape. Ultimately, the landmark analysis supports a remarkable similarity in the relative vein lengths and angle values. The results indicate that the shape shifts include proximal and distal shifts of the four secondary veins (PC1), and differences in relative lengths of the same veins (PC2). It should also be understood, however, that interpretations here concerning vein orientations based on the described landmarks will be biased to some degree. Although landmarks in all species represent the intersection of the vein trajectories and the leaf margin, only in the dissected-leafed species (*I. sloteri*, *I. quamoclit*, and *I. cairica*) do these landmarks represent the actual termination of the vein at the margin. In the simple-leafed species (*I. purpurea* and *I. coccinea*), landmarks were placed as described in order to avoid misrepresentations of the original vein trajectory, which could be potentially caused by loop-forming major veins that do not reach the margin. Future studies in this area may seek to minimize this problem by using techniques to measure and compare the full lengths of relevant major veins, rather than only attempting to measure the origin (landmark 1) and termination (landmarks 2-6), as was done here.

Also of note with regard to the landmark shapes is that along all of the remaining PC's that account for a significant amount of the total variance, all species distribution means are significantly different from one another. The most meaning that can be extracted from these likely stems from identifying species whose distribution means are most extreme along multiple PC's. For example, looking at PC's 3 and 4 combined would suggest that leaves of *I. cairica* tend toward right-handed asymmetry and that leaves of *I. sloteri* tend toward a pinching of the major secondary veins. That significant differences occur across all species along much of the remaining shape variation may point to the influences placed on the major vein arrangement by the respective laminar leaf shape. As each species considered here has a unique leaf shape, defined by the way in which the blade is dissected, the varying blade configurations could result in unique shifts in the arrangement of major veins.

With what is known about the molecular pathways leading to the initiation of vasculature, the shape similarity seen in the morphometric data likely points to a highly conserved pattern of auxin transport and response in leaves of *Ipomoea* in a manner similar to that already described. Another likely contributor to the varying leaf complexities seen here is the KNOX gene family and the level at which active members are expressed in the primordia of each

species (Burko and Ori 2013; Goliber et al. 1999; Janssen et al. 1998; Shani et al. 2009; Uchida et al. 2007). If KNOX genes function in this group similarly to how they do both in model taxa like tomato and *Arabidopsis* and in other groups (Barth et al. 2009; Bharathan et al. 2002; Champagne and Sinha 2004; Chatterjee et al. 2011; Ha et al. 2010; Hay and Tsiantis 2010; Ikezaki et al. 2010; Piazza et al. 2010; Shani et al. 2009) then we would expect, for example, that primordia of *I. quamoclit* would show re-expression leading to a prolonged state of indeterminacy which would allow for the accumulation of additional auxin maxima along the margin and, ultimately, a high degree of dissection. In this same model, simple leaf forms like that of *I. purpurea* would be achieved by continued absence of KNOX in the primordium, facilitating earlier differentiation and an entire margin due to the failure to accumulate significant auxin maxima. Investigations into the spatial and temporal expression patterns of auxin and KNOX will begin to shed light on the unique model of vein and lamina development described here.

A well supported and comprehensive phylogeny of *Ipomoea* is lacking, thus, conclusions about changes in leaf form over evolutionary timescales remain difficult. However, evidence for the conservation of complex developmental patterns, like those shown here, can provide a sense of the morphological

stability or lability present in the genus and can help, if the study system falls in a well resolved section of the clade, estimate the rate at which some characters change and when in the evolutionary past certain forms began to diverge.

## REFERENCES

- Adams DC, Rohlf FJ, and Slice DE. 2004. Geometric morphometrics: ten years of progress following the 'revolution'. *Ital J Zool* 71: 5-16
- Baima S, Possenti M, Matteucci A, Wisman E, Altamura MM, Ruberti I, and Morelli G. 2001. The *Arabidopsis* ATHB-8 HD-zip protein acts as a differentiation-promoting transcription factor of the vascular meristems. *Plant Physiol* 126 (2): 643-55
- Barkoulas M, Hay A, Kougioumoutzi E, and Tsiantis M. 2008. A developmental framework for dissected leaf formation in the *Arabidopsis* relative *Cardamine hirsuta*. *Nat Genet* 40 (9): 1136-41
- Barth S, Geier T, Eimert K, Watillon B, Sangwan RS, and Gleissberg S. 2009. KNOX overexpression in transgenic *Kohleria* (Gesneriaceae) prolongs the activity of proximal leaf blastozones and drastically alters segment fate. *Planta* 230 (6): 1081-91
- Baucom RS, Chang SM, Kniskern JM, Rausher MD, and Stinchcombe JR. 2011. Morning glory as a powerful model in ecological genomics: tracing adaptation through both natural and artificial selection. *Heredity* 107: 377-385
- Bayer EM, Smith RS, Mandel T, Nakayama N, Sauer M, Prusinkiewicz P, and Kuhlemeier C. 2009. Integration of transport-based models for phyllotaxis and midvein formation. *Genes Dev* 23 (3): 373-84
- Belles-Boix E, Hamant O, Witiak SM, Morin H, Traas J, and Pautot V. 2006. KNAT6: an *Arabidopsis* homeobox gene involved in meristem activity and organ separation. *Plant Cell* 18 (8):1900-7
- Ben-Gera H and Ori N. 2012. Auxin and LANCEOLATE affect leaf shape in tomato via different developmental processes. *Plant Signal Behav* 7 (10): 1255-1257

- Ben-Gera H, Shwartz I, Shao MR, Shani E, Estelle M, and Ori N. 2012. ENTIRE and GOBLET promote leaflet development in tomato by modulating auxin response. *Plant J* 70 (6): 903-15
- Benkova E, Michniewicz M, Sauer M, Teichmann T, Seifertova D, Jurgens G, and Friml J. 2003. Local, efflux-dependent auxin gradients as a common module for plant organ formation. *Cell* 115 (5): 591-602
- Berger Y, Harpaz-Saad S, Brand A, Melnik H, Sirding N, Alvarez JP, Zinder M, Samach A, Eshed Y, and Ori N. 2009. The NAC-domain transcription factor GOBLET specifies leaflet boundaries in compound tomato leaves. *Development* 136 (5): 823-32
- Bharathan G, Goliber TE, Moore C, Kessler S, Pham T, and Sinha NR. 2002. Homologies in leaf form inferred from KNOXI gene expression during development. *Science* 296 (5574): 1858-1860
- Bilsborough GD, Runions A, Barkoulas M, Jenkins HW, Hasson A, Galinha C, Laufs P, Hay A, Prusinkiewicz P, and Tsiantis M. 2011. Model for the regulation of *Arabidopsis thaliana* leaf margin development. *Proc Natl Acad Sci U S A* 108 (8): 3424-9
- Bowman JL. 2000. Axial patterning in leaves and other lateral organs. *Current Opinion in Plant Biology* 10: 399-404
- Bright KL, and Rausher MD. 2008. Natural selection on a leaf-shape polymorphism in the ivyleaf morning glory (*Ipomoea hederacea*). *Evolution* 62 (8): 1978-1990
- Burko Y and Ori N. 2013. The tomato as a model system for organogenesis. *Methods Mol Biol* 959: 1-19
- Campitelli BE, Gorton AJ, Ostevik KL, and Stinchcombe JR. 2013. The effect of leaf shape on the thermoregulation and frost tolerance of an annual vine, *Ipomoea hederacea* (Convolvulaceae). *Am J Bot* 100 (11): 2175-2182

- Campitelli BE and Stinchcombe JR. 2013a. Natural selection maintains a single-locus leaf shape cline in Ivyleaf morning glory, *Ipomoea hederacea*. *Molecular Ecology* 22: 552-564
- Campitelli BE and Stinchcombe JR. 2013b. Testing potential selective agents acting on leaf shape in *Ipomoea hederacea*: predictions based on an adaptive leaf shape cline. *Ecology and Evolution* 3 (8): 2409-2423
- Canales C, Barkoulas M, Galinha C, and Tsiantis M. 2010. Weeds of change: *Cardamine hirsuta* as a new model system for studying dissected leaf development. *J Plant Res* 123 (1): 25-33
- Champagne CE, Goliber TE, Wojciechowski MF, Mei RW, Townsley BT, Wang K, Paz MM, Geeta R, and Sinha NR. 2007. Compound leaf development and evolution in the legumes. *Plant Cell* 19 (11): 3369-78
- Champagne C and Sinha N. 2004. Compound leaves: equal to the sum of their parts? *Development* 131 (18): 4401-12
- Chatterjee M, Bermudez-Lozano CL, Clancy MA, Davis TM, and Folta KM. 2011. A strawberry KNOX gene regulates leaf, flower and meristem architecture. *PLoS One* 6: e24752
- Chen MK, Wilson RL, Palme K, Ditengou FA, and Shpak ED. 2013. ERECTA family genes regulate auxin transport in the shoot apical meristem and forming leaf primordia. *Plant Physiol* 162 (4): 1978-1991
- Chitwood DH, Guo M, Nogueira FT, and Timmermans MC. 2007. Establishing leaf polarity: the role of small RNAs and positional signals in the shoot apex. *Development* 134 (5): 813-23
- Chitwood DH, Headland LR, Filaault DL, Kumar R, Jimenez-Gomez JM, Schragger AV, Park DS, Peng J, Sinha NR, and Maloof JN. 2012. Native environment modulates leaf size and response to simulated foliar shade across wild tomato species. *PLoS One* 7 (1): e29570

- Chitwood DH, Headland LR, Kumar R, Peng J, Maloof JN, and Sinha NR. 2012. The developmental trajectory of leaflet morphology in wild tomato species. *Plant Physiol* 158 (3): 1230-40
- Chitwood DH, Headland LR, Ranjan A, Martinez CC, Braybrook SA, Koenig DP, Kuhlemeier C, Smith RS, and Sinha NR. 2012. Leaf asymmetry as a developmental constraint imposed by auxin-dependent phyllotactic patterning. *Plant Cell* 24 (6): 2318-27
- Chitwood DH, Naylor DT, Thammapichai P, Weeger AC, Headland LR, and Sinha NR. 2012. Conflict between Intrinsic Leaf Asymmetry and Phyllotaxis in the Resupinate Leaves of *Alstroemeria psittacina*. *Front Plant Sci* 3: 182
- Chitwood DH, Ranjan A, Martinez CC, Headland LR, Thiem T, Kumar R, Covington MF, Hatcher T, Naylor DT, Zimmerman S, et al. 2014. A modern ampelography: a genetic basis for leaf shape and venation patterning in grape. *Plant Physiol* 164 (1): 259-272
- David-Schwartz R, Koenig D, and Sinha NR. 2009. LYRATE is a key regulator of leaflet initiation and lamina outgrowth in tomato. *Plant Cell* 21 (10): 3093-104
- DeMason DA and Chawla R. 2004. Roles for auxin during morphogenesis of the compound leaves of pea (*Pisum sativum*). *Planta* 218 (3): 435-48
- DeMason DA and Chetty VJ. 2011. Interactions between GA, auxin, and UNI expression controlling shoot ontogeny, leaf morphogenesis, and auxin response in *Pisum sativum* (Fabaceae): or how the uni-tac mutant is rescued. *Am J Bot* 98: 775-791
- Dengler N and Kang J. 2001. Vascular patterning and leaf shape. *Curr Opin Plant Biol* 4 (1): 50-6
- Donner TJ, Sherr I, and Scarpella E. 2009. Regulation of preprocambial cell state acquisition by auxin signaling in *Arabidopsis* leaves. *Development* 136 (19): 3235-46

- Donner TJ, Sherr I, and Scarpella E. 2010. Auxin signal transduction in *Arabidopsis* vein formation. *Plant Signal Behav* 5 (1)
- Efroni I, Blum E, Goldshmidt A, and Eshed Y. 2008. A protracted and dynamic maturation schedule underlies *Arabidopsis* leaf development. *Plant Cell* 20 (9): 2293-306
- Efroni I, Eshed Y, and Eliezer L. 2010. Morphogenesis of Simple and Compound Leaves: A Critical Review. *The Plant Cell* 22: 1019-1032
- Emery JF, Floyd SK, Alvarez J, Eshed Y, Hawker NP, Izhaki A, Baum SF, and Bowman JL. 2003. Radial patterning of *Arabidopsis* shoots by class III HD-ZIP and KANADI genes. *Curr Biol* 13 (20): 1768-74
- Eshed Y, Izhaki A, Baum SF, Floyd SK, and Bowman JL. 2004. Asymmetric leaf development and blade expansion in *Arabidopsis* are mediated by KANADI and YABBY activities. *Development* 131 (12): 2997-3006
- Fleming AJ, Mandel T, Roth I, and Kuhlemeier C. 1993. The patterns of gene expression in the tomato shoot apical meristem. *Plant Cell* 5 (3): 297-309
- Galweiler L, Guan C, Muller A, Wisman E, Mendgen K, Yephremov A, and Palme K. 1998. Regulation of polar auxin transport by AtPIN1 in *Arabidopsis* vascular tissue. *Science* 282 (5397): 2226-30
- Gardiner J, Donner TJ, and Scarpella E. 2011. Simultaneous activation of SHR and ATHB8 expression defines switch to preprocambial cell state in *Arabidopsis* leaf development. *Dev Dyn* 240 (1): 261-70
- Garrett JJ, Meents MJ, Blackshaw MT, Blackshaw LC, Hou H, Styranko DM, Kohalmi SE, and Schultz EA. 2012. A novel, semi-dominant allele of MONOPTEROS provides insight into leaf initiation and vein pattern formation. *Planta* 236: 297-312
- Geeta R, Davalos LM, Levy AA, Bohs L, Lavin M, Mummenhoff K, Sinha N, and Wojciechowski MF. 2012. Keeping it simple: flowering plants tend to retain, and revert to, simple leaves. *New Phytol* 193: 481-493

- Givnish TJ and Vermeij GT. 1976. Sizes and Shapes of Liane Leaves. *Am Nat* 110 (975): 743-778
- Gleissberg S. 1998. Comparative analysis of leaf shape development in Papaveraceae-Papaveroideae. *Flora (Jena)* 193 (3): 269-301
- Gleissberg S. 2004. Comparative analysis of leaf shape development in *Eschscholzia californica* and other Papaveraceae-Eschscholzioideae. *Am J Bot* 91: 306-312
- Gleissberg S and Kadereit JW. 1999. Evolution of leaf morphogenesis: Evidence from developmental and phylogenetic data in Papaveraceae. *Int J Plant Sci* 160 (4): 787-794
- Goliber T, Kessler S, Chen JJ, Bharathan G, and Sinha N. 1999. Genetic, molecular, and morphological analysis of compound leaf development. *Curr Top Dev Biol* 43: 259-90
- Gourlay CW, Hofer JM, and Ellis TH. 2000. Pea compound leaf architecture is regulated by interactions among the genes UNIFOLIATA, COCHLEATA, AFILA, and TENDRIL-LESS. *Plant Cell* 12 (8): 1279-94
- Grigg SP, Canales C, Hay A, and Tsiantis M. 2005. SERRATE coordinates shoot meristem function and leaf axial patterning in *Arabidopsis*. *Nature* 437 (7061): 1022-6
- Groot EP, Sinha N, and Gleissberg S. 2005. Expression patterns of STM-like KNOX and Histone H4 genes in shoot development of the dissected-leaved basal eudicot plants *Chelidonium majus* and *Eschscholzia californica* (Papaveraceae). *Plant Mol Biol* 58 (3): 317-31
- Ha CM, Jun JH, and Fletcher JC. 2010. Control of *Arabidopsis* leaf morphogenesis through regulation of the YABBY and KNOX families of transcription factors. *Genetics* 186 (1): 197-206

- Hagemann W and Gleissberg S. 1996. Organogenetic capacity of leaves: the significance of marginal blastozones in angiosperms. *Plant Syst Evol* 199: 121-152
- Hasson A, Plessis A, Blein T, Adroher B, Grigg S, Tsiantis M, Boudaoud A, Damerval C, and Laufs P. 2011. Evolution and diverse roles of the CUP-SHAPED COTYLEDON genes in *Arabidopsis* leaf development. *Plant Cell* 23 (1): 54-68
- Hay A, Barkoulas M, and Tsiantis M. 2006. ASYMMETRIC LEAVES1 and auxin activities converge to repress BREVIPEDICELLUS expression and promote leaf development in *Arabidopsis*. *Development* 133 (20): 3955-61
- Hay A and Tsiantis M. 2009. A KNOX family TALE. *Curr Opin Plant Biol* 12 (5): 593-8
- Hay A and Tsiantis M. 2010. KNOX genes: versatile regulators of plant development and diversity. *Development* 137 (19): 3153-65
- Hofer J, Turner L, Hellens R, Ambrose M, Matthews P, Michael A, and Ellis N. 1997. UNIFOLIATA regulates leaf and flower morphogenesis in pea. *Curr Biol* 7 (8): 581-7
- Ikezaki M, Kojima M, Sakakibara H, Kojima S, Ueno Y, Machida C, and Machida Y. 2010. Regulation of SHOOT MERISTEMLESS genes via an upstream-conserved noncoding sequence coordinates leaf development. *Plant J* 61:70-82
- Ilegems M, Douet V, Meylan-Bettex M, Uyttewaal M, Brand L, Bowman JL, and Stieger PA. 2010. Interplay of auxin, KANADI and Class III HD-ZIP transcription factors in vascular tissue formation. *Development* 137 (6): 975-84
- Jackson D, Veit B, and Hake S. 1994. Expression of maize *KNOTTED 1* related homeobox genes in the shoot apical meristem predicts patterns of morphogenesis in the vegetative shoot. *Development* 120: 405-413

- Janssen BJ, Lund L, and Sinha N. 1998. Overexpression of a homeobox gene, LeT6, reveals indeterminate features in the tomato compound leaf. *Plant Physiol* 117 (3): 771-86
- Janssen BJ, Williams A, Chen JJ, Mathern J, Hake S, and Sinha N. 1998. Isolation and characterization of two knotted-like homeobox genes from tomato. *Plant Mol Biol* 36 (3): 417-25
- Jasinski S, Kaur H, Tattersall A, and Tsiantis M. 2007. Negative regulation of KNOX expression in tomato leaves. *Planta* 226 (5): 1255-63
- Jones CS, Bakker FT, Schlichting CD, and Nicotra AB. 2009. Leaf shape evolution in the South African genus *Pelargonium* L' Her. (Geraniaceae). *Evolution* 63 (2): 479-497
- Jones AW, Doughan BG, Gerrath JM, and Kang J. 2013. Development of leaf shape in two North American native species of *Ampelopsis* (Vitaceae). *Can J Bot* 91 (12): 857-865
- Kang J and Dengler N. 2002. Cell cycling frequency and expression of the homeobox gene ATHB-8 during leaf vein development in *Arabidopsis*. *Planta* 216 (2): 212-9
- Kang J and Dengler N. 2004. Vein pattern development in adult leaves of *Arabidopsis thaliana*. *Int J Plant Sci* 165 (2): 231-242
- Kang J and Dengler N. 2005. Leaf architecture - regulation of leaf position, shape, and internal structure. In: Turnbull CGN. *Plant Architecture and its Manipulation*. CRC Press. p. 322
- Kang J and Sinha N. 2010. Leaflet initiation is temporally and spatially separated in simple and complex tomato (*Solanum lycopersicum*) leaf mutants: a developmental analysis. *Botany* 88: 710-724
- Kaplan DR, Dengler NG, and Dengler RE. 1982. The mechanisms of plication inception in palm leaves: Histogenetic observations of the palmate leaves of *Rhapis excelsa*. *Can. J. Bot.* 60: 2999-3016

- Kerstetter RA., Laudencia-Chingcuanco D, Smith LG, and Hake S. 1997. Loss-of-function mutations in the maize homeobox gene, *knotted1*, are defective in shoot meristem maintenance. *Development (Cambridge)* 124 (16): 3045-3054
- Kim JY, Yuan Z, and Jackson D. 2003. Developmental regulation and significance of KNOX protein trafficking in *Arabidopsis*. *Development* 130 (18): 4351-62
- Kim M, McCormick S, Timmermans M, and Sinha N. 2003. The expression domain of PHANTASTICA determines leaflet placement in compound leaves. *Nature* 424 (6947): 438-43
- Kim M, Pham T, Hamidi A, McCormick S, Kuzoff RK, and Sinha N. 2003. Reduced leaf complexity in tomato wiry mutants suggests a role for PHAN and KNOX genes in generating compound leaves. *Development* 130 (18): 4405-15
- Klingenberg CP, Duttke S, Whelan S, and Kim M. 2012. Developmental plasticity, morphological variation and evolvability: a multilevel analysis of morphometric integration in the shape of compound leaves. *J Evol Biol* 25 (1): 115-129
- Koenig D, Bayer E, Kang J, Kuhlemeier C, and Sinha N. 2009. Auxin patterns *Solanum lycopersicum* leaf morphogenesis. *Development* 136 (17): 2997-3006
- Koltai H and Bird DM. 2000. Epistatic repression of PHANTASTICA and class 1 KNOTTED genes is uncoupled in tomato. *Plant Journal* 22 (5): 455-459
- Kuhlemeier C, Fleming AJ, and Mandel T. 1993. The patterns of gene expression in the vegetative shoot apical meristem. *Journal of Cellular Biochemistry Supplement* 0 (17 PART B): 30
- Kuhlemeier C and Reinhardt D. 2001. Auxin and phyllotaxis. *Trends Plant Sci* 6 (5):187-189

- Long JA, Moan EI, Medford JI, and Barton MK. 1996. A member of the KNOTTED class of homeodomain proteins encoded by the *STM* gene of *Arabidopsis*. *Nature* 379 (6560): 66-9
- Long JA, McConnell J, Fernandez A, Grbic V, and Barton MK. 1996. Developmental genetics of shoot apical meristem formation in *Arabidopsis*. *Plant Physiol* 111 (2 SUPPL.): 12
- Manos PS, Miller RE, and Wilkin P. 2001. Phylogenetic Analysis of *Ipomoea*, *Argyrea*, *Stictocardia*, and *Turbina* Suggests a Generalized Model of Morphological Evolution in Morning Glories. *Systematic Botany* 26 (3): 585-602
- Mattsson J, Sung RZ, and Berleth T. 1999. Responses of plant vascular systems to auxin transport inhibition. *Development* 126: 2979-2991
- Mattsson J, Ckurshumova W, and Berleth T. 2003. Auxin signaling in *Arabidopsis* leaf vascular development. *Plant Physiol* 131 (3): 1327-39
- McConnell JR, Emery J, Eshed Y, Bao N, Bowman J, and Barton MK. 2001. Role of PHABULOSA and PHAVOLUTA in determining radial patterning in shoots. *Nature* 411: 709-713
- McHale NA, and Koning RE. 2004. PHANTASTICA regulates development of the adaxial mesophyll in *Nicotiana* leaves. *Plant Cell* 16 (5): 1251-1262
- McKown AD, Cochard H, and Sack L. 2010. Decoding leaf hydraulics with a spatially explicit model: principles of venation architecture and implications for its evolution. *Am Nat* 175 (4): 447-460
- Mele G, Ori N, Sato Y, and Hake S. 2003. The knotted1-like homeobox gene BREVIPEDICELLUS regulates cell differentiation by modulating metabolic pathways. *Genes Dev* 17 (17): 2088-93
- Miller RE, McDonald JA, and Manos PS. 2004. Systematics of *Ipomoea* subgenus *Quamoclit* (Convolvulaceae) based on ITS sequence data and a bayesian phylogenetic analysis. *Am J Bot* 91 (8): 1208-1218

- Nakayama N and Kuhlemeier C. 2009. Leaf development: untangling the spirals. *Curr Biol* 19 (2): R71-4
- Nelson T and Dengler N. 1997. Leaf vascular pattern formation. *Plant Cell* 9: 1121-1135
- Nicotra AB, Leigh A, Boyce CK, Jones CS, Niklas KJ, Royer DL, and Tsukaya H. 2011. The evolution and functional significance of leaf shape in the angiosperms. *Functional Plant Biology* 38: 535-552
- Nikovics K, Blein T, Peaucelle A, Ishida T, Morin H, Aida M, and Laufs P. 2006. The balance between the MIR164A and CUC2 genes controls leaf margin serration in *Arabidopsis*. *Plant Cell* 18 (11): 2929-45
- Nowak, J. S., N. Bolduc, N. G. Dengler, and U. Posluszny. 2011. Compound leaf development in the palm *Chamaedorea elegans* is KNOX-independent. *Am J Bot* 98 (10): 1575-82
- Ori N, Cohen AR, Etzioni A, Brand A, Yanai O, Shleizer S, Menda N, Amsellem Z, Efroni I, Pekker I, et al. 2007. Regulation of LANCEOLATE by miR319 is required for compound-leaf development in tomato. *Nat Genet* 39 (6): 787-91
- Ori N, Eshed Y, Chuck G, Bowman JL, and Hake S. 2000. Mechanisms that control knox gene expression in the *Arabidopsis* shoot. *Development* 127 (24): 5523-5532
- Peaucelle A, Morin H, Traas J, and Laufs P. 2007. Plants expressing a miR164-resistant CUC2 gene reveal the importance of post-meristematic maintenance of phyllotaxy in *Arabidopsis*. *Development* 134 (6): 1045-50
- Perez-Perez JM, Rubio-Diaz S, Dhondt S, Hernandez-Romero D, Sanchez-Soriano J, Beemster GTS, Ponce MR, and Micol JL. 2011. Whole organ, venation and epidermal cell morphological variations are correlated in the leaves of *Arabidopsis* mutants. *Plant, Cell & Environment* 34: 2200-2211

- Piazza P, Bailey CD, Cartolano M, Krieger J, Cao J, Ossowski S, Schneeberger K, He F, de Meaux J, Hall N, et al. 2010. *Arabidopsis thaliana* leaf form evolved via loss of KNOX expression in leaves in association with a selective sweep. *Curr Biol* 20 (24): 2223-8
- Reinhardt D, Mandel T, and Kuhlemeier C. 2000. Auxin regulates the initiation and radial position of plant lateral organs. *Plant Cell* 12 (4): 507-518
- Reinhardt D, Pesce ER, Stieger P, Mandel T, Baltensperger K, Bennett M, Traas J, Friml J, and Kuhlemeier C. 2003. Regulation of phyllotaxis by polar auxin transport. *Nature* 426 (6964): 255-60
- Roth-Nebelsick A, Uhl D, Mosbrugger V, Kerp H. 2001. Evolution and function of leaf venation architecture: A review. *Ann Bot* 87: 553-566
- Sack L and Scoffoni C. 2013. Leaf venation: structure, function, development, evolution, ecology and applications in the past, present and future. *New Phytol* 198 (4): 983-1000
- Sawchuck MG, Donner TJ, and Scarpella E. 2008. Auxin transport-dependent, stage-specific dynamics of leaf vein formation. *Plant Signal Behav* 3: 286-289
- Sawchuk MG, Edgar A, and Scarpella E. 2013. Patterning of leaf vein networks by convergent auxin transport pathways. *PLoS Genet* 9 (2): e1003294.
- Sawchuck T, Head P, Donner TJ, and Scarpella E. 2007. Time lapse imaging of *Arabidopsis* leaf development shows dynamic patterns of procambium formation. *New Phytol* (176): 560-571
- Scanlon MJ. 2000. Developmental complexities of simple leaves. *Curr Opin Plant Biol* 3: 31-36
- Scanlon, MJ. 2003. The polar auxin transport inhibitor N-1-naphthylphthalamic acid disrupts leaf initiation, KNOX protein regulation, and formation of leaf margins in maize. *Plant Physiol* 133 (2): 597-605

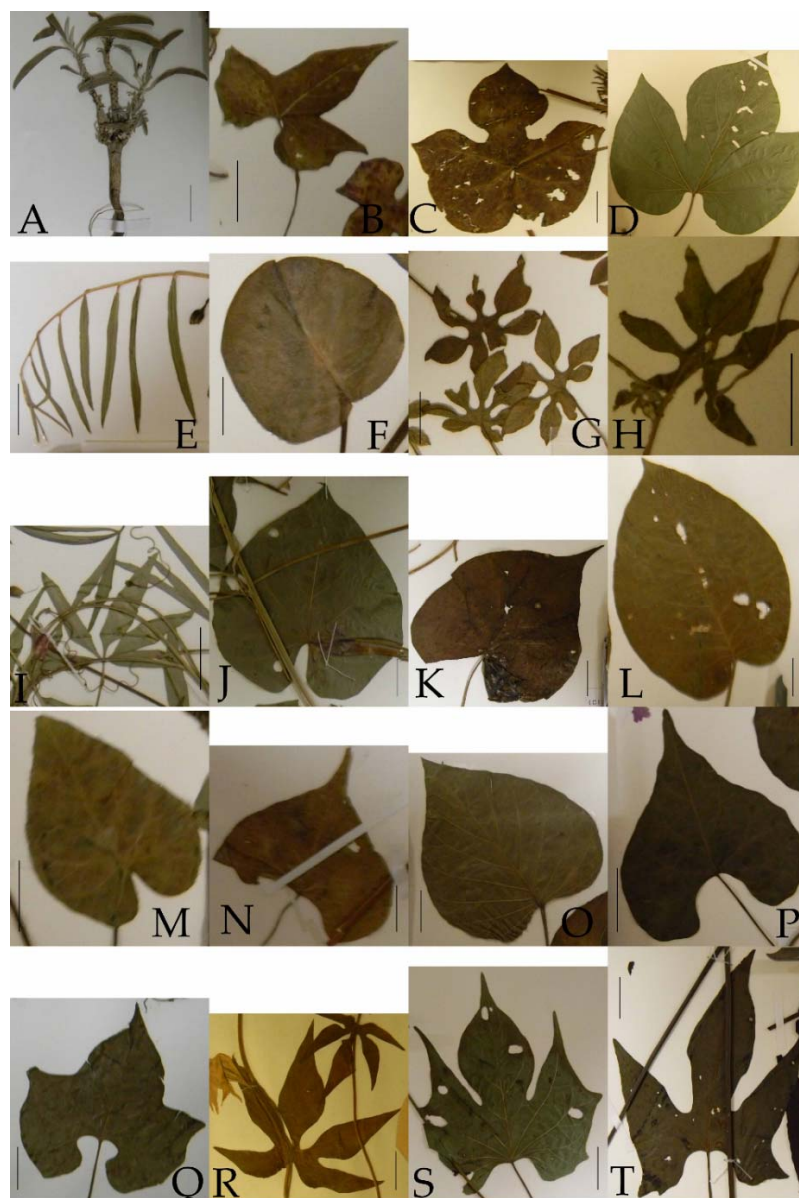
- Scarpella E, Barkoulas M, and Tsiantis M. 2010. Control of leaf and vein development by auxin. *Cold Spring Harb Perspect Biol* 2 (1): a001511
- Scarpella E, Francis P, and Berleth T. 2004. Stage-specific markers define early steps of procambium development in *Arabidopsis* leaves and correlate termination of vein formation with mesophyll differentiation. *Development* 131 (14): 3445-55
- Scarpella E, Marcos D, Friml J, and Berleth T. 2006. Control of leaf vascular patterning by polar auxin transport. *Genes & Development* (20): 1015-1027
- Scoffoni C, Rawls A, McKown AD, Cochard H, and Sack L. 2011. Decline of leaf hydraulic conductance with dehydration: relationship to leaf size and venation architecture. *Plant Physiol* 156 (2): 832-843
- Shani E, Burko Y, Ben-Yaakov L, Berger Y, Amsellem Z, Goldshmidt A, Sharon E, and Ori N. 2009. Stage-specific regulation of *Solanum lycopersicum* leaf maturation by class 1 KNOTTED1-LIKE HOMEODOMAIN proteins. *Plant Cell* 21: 3078-3092
- Shleizer-Burko S, Burko Y, Ben-Herzel O, and Ori N. 2011. Dynamic growth program regulated by LANCEOLATE enables flexible leaf patterning. *Development* 138: 695-704
- Siegfried KR., Eshed Y, Baum SF, Otsuga D, Drews GN, and Bowman JL. 1999. Members of the YABBY gene family specify abaxial cell fate in *Arabidopsis*. *Development (Cambridge)* 126 (18): 4117-4128
- Sinha N, Williams RE, and Hake S. 1993. Overexpression of the maize homeobox gene, *KNOTTED-1*, cause a switch from determinate to indeterminate cell fates. *Genes and Development* 7: 787-795
- Slice DE. 2001. Landmark Coordinates Aligned by Procrustes Analysis Do Not Lie in Kendall's Shape Space. *Syst Biol* 50 (1): 141-149

- Smith LG, Greene B, Veit B, and Hake S. 1992. A dominant mutation in the maize homeobox gene, *Knotted-1*, causes its ectopic expression in leaf cells with altered fates. *Development* 116 (1): 21-30
- Sousa-Baena MS, Lohmann LG, Rossi M, and Sinha NR. 2014. Acquisition and diversification of tendrilled leaves in Bignoniaceae (Bignoniaceae) involved changes in expression patterns of *SHOOTMERISTEMLESS* (*STM*), *LEAFY/FLORICAULA* (*LFY/FLO*), and *PHANTASTICA* (*PHAN*). *New Phytol* 201 (3): 993-1008
- Spinelli SV, Martin AP, Viola RL, Gonzalez DH, and Palatnik JF. 2011. A mechanistic link between *STM* and *CUC1* during *Arabidopsis* development. *Plant Physiol* 156: 1894-1904
- Stefanovic S, Krueger L, and Olmstead RG. 2002. Monophyly of the Convolvulaceae and circumscription of their major lineages based on DNA sequences of multiple chloroplast loci. *Am J Bot* 89 (9): 1510-1522
- Stieger PA, Reinhardt D, and Kuhlemeier C. 2002. The auxin influx carrier is essential for correct leaf positioning. *Plant J* 32 (4): 509-17
- Sylvester AW, Parker-Clark V, and Murray GA. 2001. Leaf shape and anatomy as indicators of phase change in the grasses: comparison of maize, rice, and bluegrass. *Am J Bot* 88 (12): 2157-2167
- Telfer A, Bollman KM, and Poethig RS. 1997. Phase change and the regulation of trichome distribution in *Arabidopsis thaliana*. *Development* 124 (3): 645-654
- Tsiantis M, Brown MI, Skibinski G, and Langdale JA. 1999. Disruption of auxin transport is associated with aberrant leaf development in maize. *Plant Physiol* 121 (4): 1163-8
- Tsukaya H. 2005. Leaf shape: genetic controls and environmental factors. *Int J Dev Biol* 49: 547-555

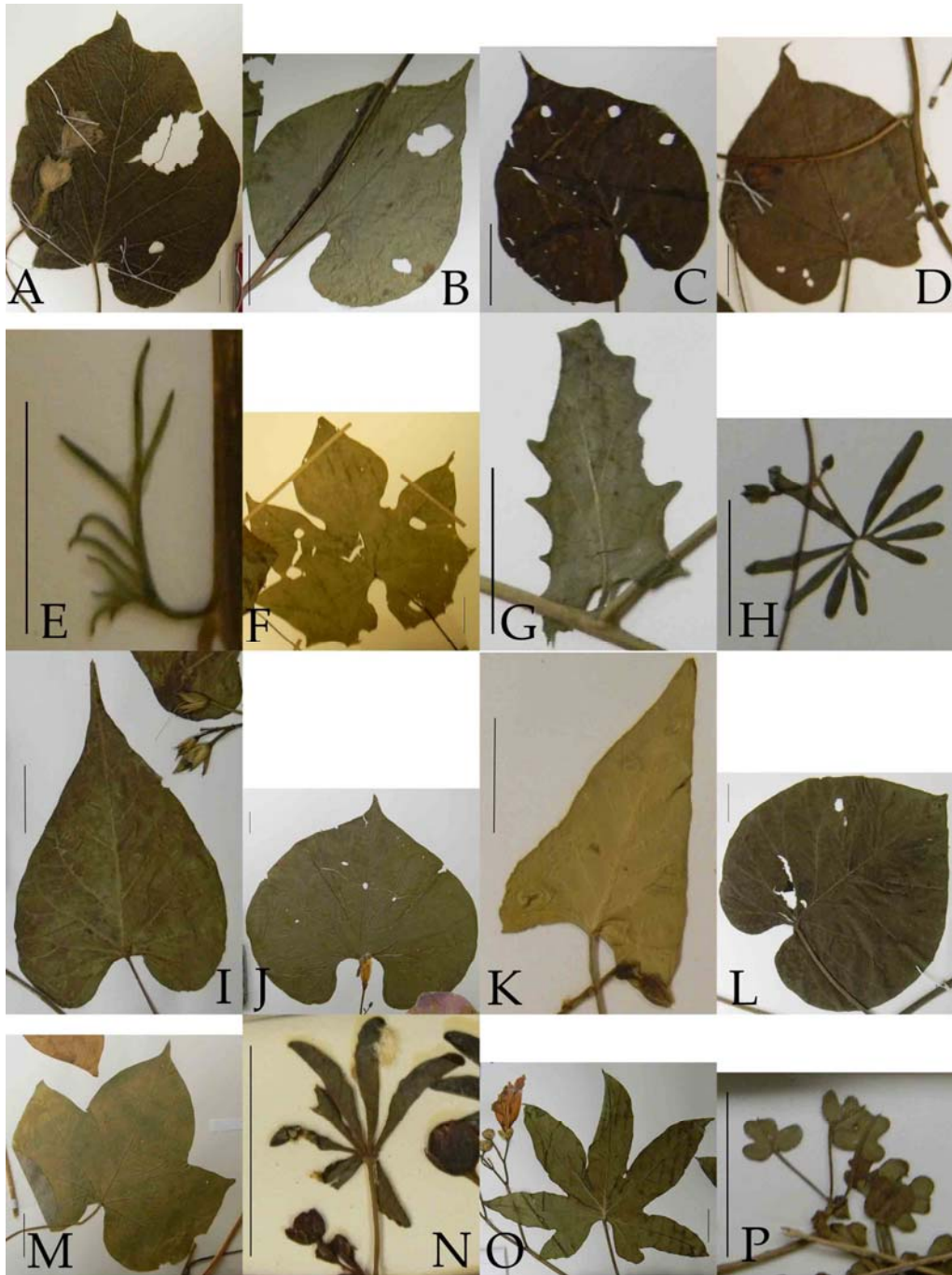
- Uchida N, Townsley B, Chung KH, and Sinha N. 2007. Regulation of *SHOOT MERISTEMLESS* genes via an upstream-conserved noncoding sequence coordinates leaf development. *Proc Natl Acad Sci U S A* 104 (40): 15953-15958
- Venglat SP, Dumonceaux T, Rozwadowski K, Parnell L, Babic V, Keller W, Martienssen R, Selvaraj G, and Datla R. 2002. The homeobox gene *BREVIPEDICELLUS* is a key regulator of inflorescence architecture in *Arabidopsis*. *Proc Natl Acad Sci U S A* 99 (7): 4730-5
- Viscosi V and Cardini A. 2011. Leaf Morphology, Taxonomy and Geometric Morphometrics: A Simplified Protocol for Beginners. *PLoS One* no. 6 (10): 1-20
- Vlad D, Kierzkowski D, Rast MI, Vuolo F, Ioio RD, Galinha C, Gan X, Hajheidari M, Hay A, Smith RS, et al. 2014. Leaf shape evolution through duplication, regulatory diversification, and loss of a homeobox gene. *Science* 343:780-783
- Vollbrecht E, Veit B, Sinha N, and Hake S. 1990. The developmental gene *Knotted-1* is a member of a maize homeobox gene family. *Nature* 350: 241-43
- Waites R and Hudson A. 1995. Phantastica: a gene required for dorsoventrality of leaves in *Antirrhinum majus*. *Development* 121: 2143-2154
- Waites R, Selvadurai HRN, Oliver IR, and Hudson A. 1998. The Phantastica gene encodes a MYB transcription factor involved in growth and dorsoventrality of lateral organs in *Antirrhinum*. *Cell* 93: 779-89
- Wenzel CL, Schuetz M, Yu Q, and Mattsson J. 2007. Dynamics of *MONOPTEROS* and *PIN-FORMED1* expression during leaf vein pattern formation in *Arabidopsis thaliana*. *Plant J* 49 (3): 387-98
- Zoulias N, Koenig D, Hamidi A, McCormick S, and Kim M. 2012. A role for *PHANTASTICA* in medio-lateral regulation of adaxial domain development in tomato and tobacco leaves. *Ann Bot* 109 (2): 407-418

## APPENDIX

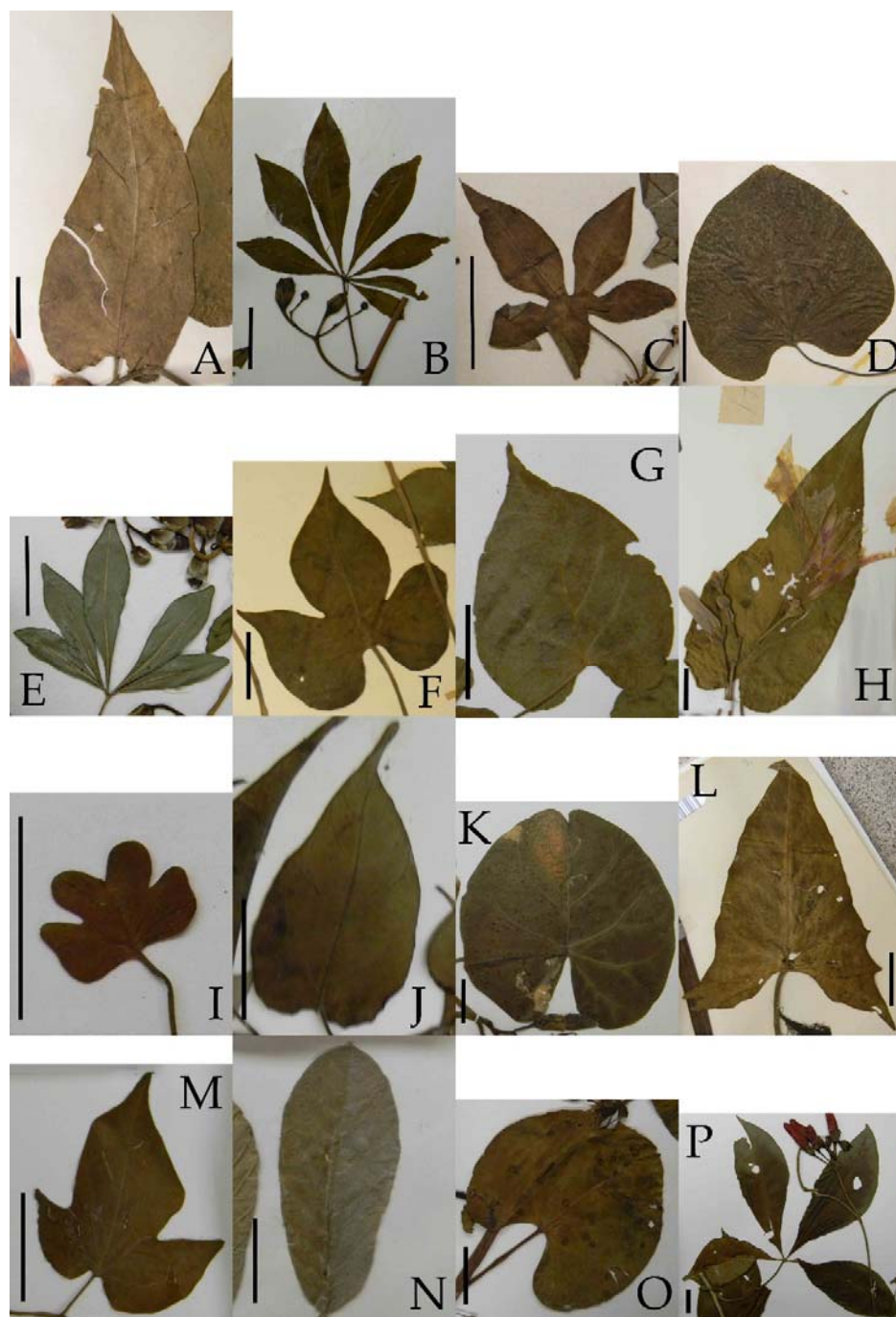
## HERBARIUM LEAF SAMPLES



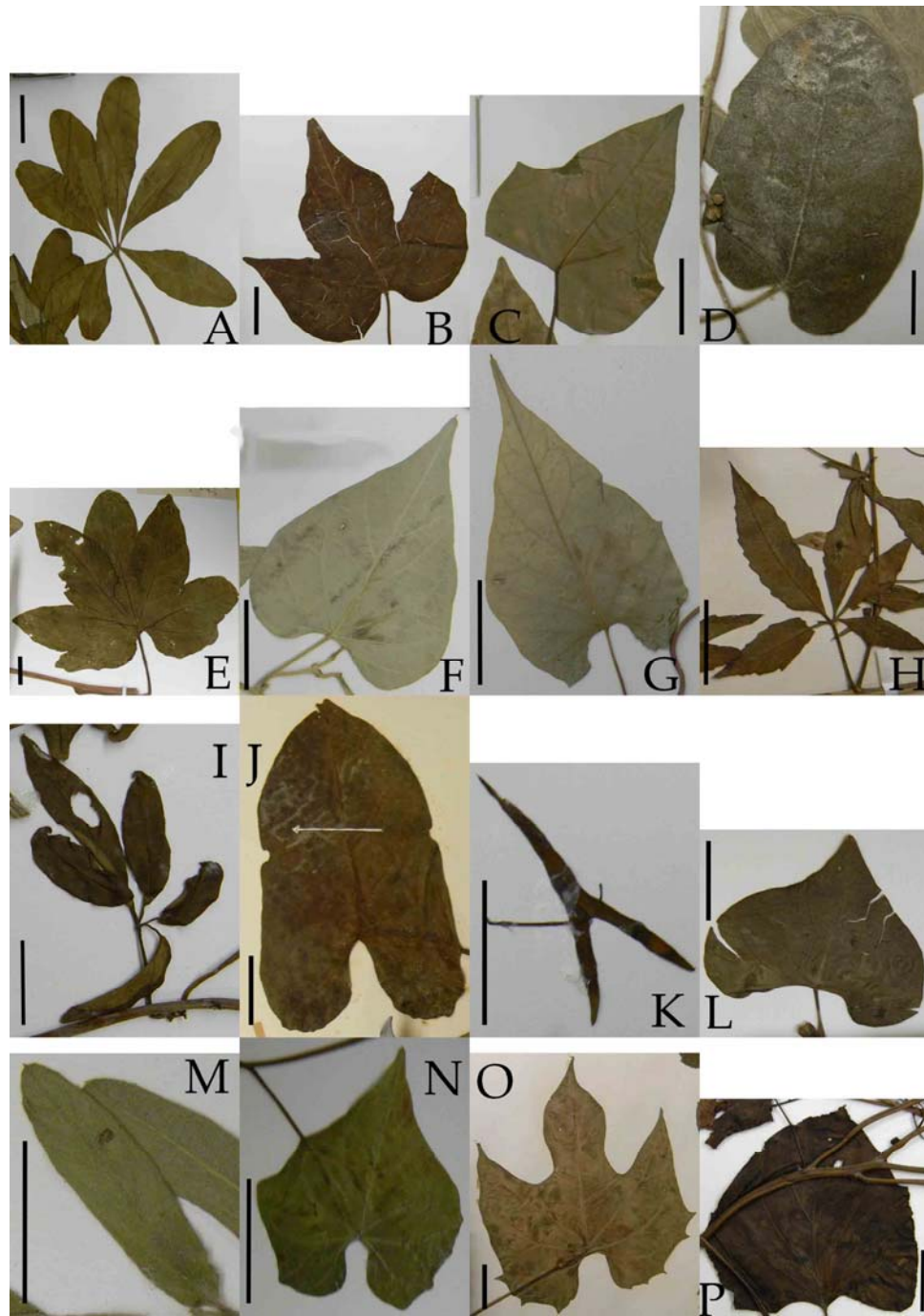
Leaf shapes across *Ipomoea* (A) *I. jaegeri* (B) *I. cordatotriloba* (C) *I. hederacea* (D) *I. indica* (E) *I. leptophylla* (F) *I. pes-caprae* (G) *I. pes-tigridis* (H) *I. pubescens* (I) *I. wrightii* (J) *I. turbinata* (K) *I. alba* (L) *I. arborescens* (M) *I. batatas* (N) *I. cardiophylla* (O) *I. carnea* (P) *I. crinalyx* (Q) *I. hederifolia* (R) *I. Lindheimeri* (S) *I. lutea* (T) *I. neei*. Scale Bars: 2cm. All images taken by the author from material at the Missouri Botanical Garden Herbarium with permission from Dr. Jim Solomon, Curator.



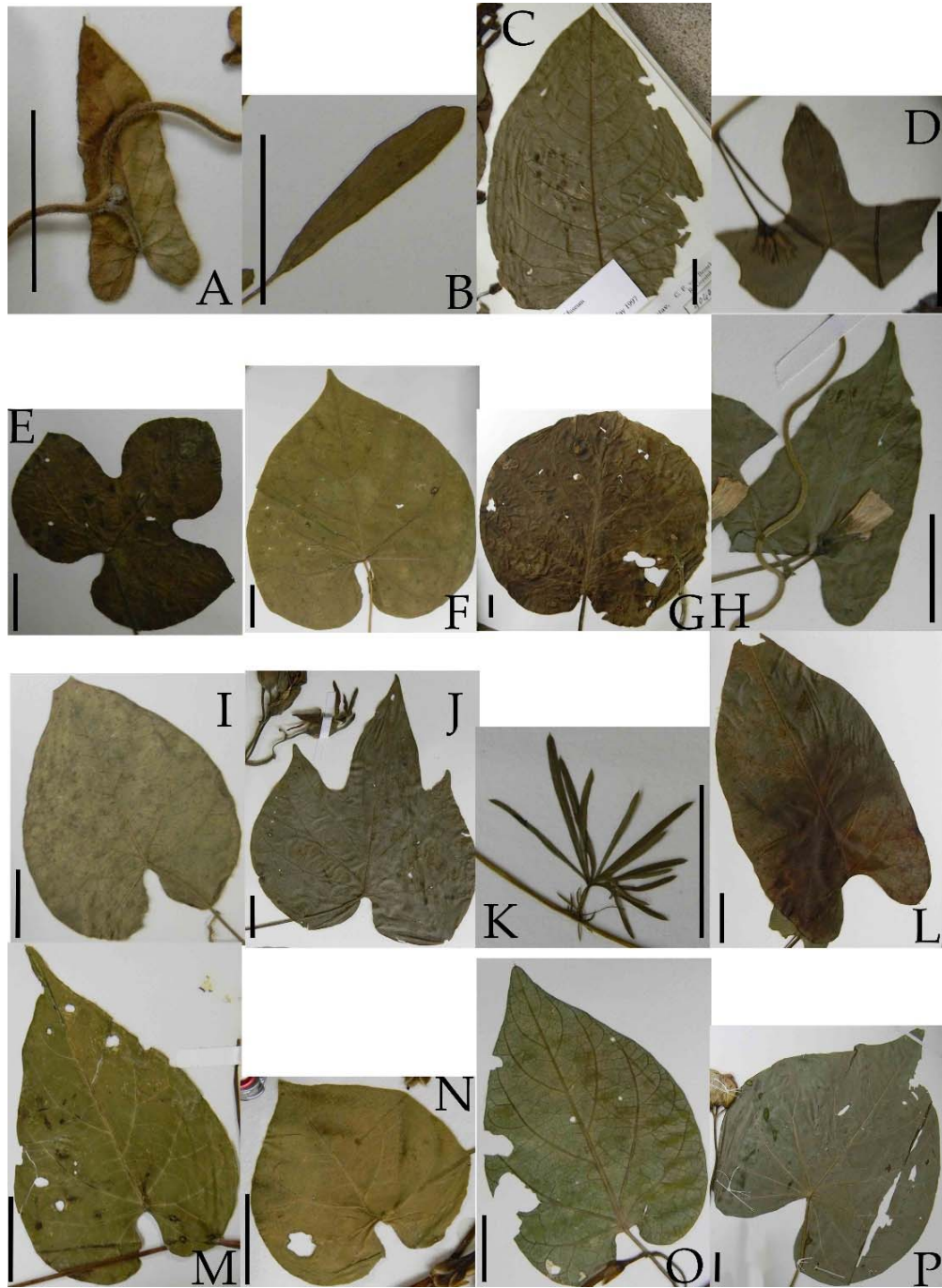
Leaf shapes across *Ipomoea* (A) *I. neurocephala* (B) *I. orizabensis* (C) *I. parasitica* (D) *I. rubens* (E) *I. sescosiana* (F) *I. setosa* (G) *I. stans* (H) *I. ternifolia* (I) *I. tiliacea* (J) *I. tricolor* (K) *I. aquatica* (L) *I. mairetii* (M) *I. nil* (N) *I. desrousseauxii* (O) *I. digitata* (P) *I. eggersii*. Scale Bars: 2cm. All images taken by the author from material at the Missouri Botanical Garden Herbarium with permission from Dr. Jim Solomon, Curator.



Leaf shapes across *Ipomoea* (A) *I. fistulosa* (B) *I. furcyensis* (C) *I. cavanillesii* (D) *I. calantha* (E) *I. carolina* (F) *I. cathartica* (G) *I. corymbosa* (H) *I. crassicaulis* (I) *I. crenaria* (J) *I. cyanantha* (K) *I. aculeatum* (L) *I. aquatica* (M) *I. arenaria* (N) *I. argentifolia* (O) *I. asarifolia* (P) *I. horsfalliae*. Scale Bars: 2cm. All images taken by the author from material at the Missouri Botanical Garden Herbarium with permission from Dr. Jim Solomon, Curator.



Leaf shapes across *Ipomoea* (A) *I. heptophylla* (B) *I. jamaicensis* (C) *I. triloba* (D) *I. luteo-viridis* (E) *I. mauritiana* (F) *I. ochracea* (G) *I. praematura* (H) *I. quinquefolia* (I) *I. rubella* (J) *I. rubra* (K) *I. sagittata* (L) *I. amnicola* (M) *I. cuneifolia* (N) *I. dumetorum* (O) *I. lobata* (P) *I. umbraticola* Scale Bars: 2cm. All images taken by the author from material at the Missouri Botanical Garden Herbarium with permission from Dr. Jim Solomon, Curator.



Leaf shapes across *Ipomoea* (A) *I. eriocarpa* (B) *I. polymorpha* (C) *I. sumatrana* (D) *I. sepiaria* (E) *I. arachnosperma* (F) *I. seducta* (G) *I. kituiensis* (H) *I. plebeia* (I) *I. obscura* (J) *I. ampullacea* (K) *I. chamelana* (L) *I. funis* (M) *I. hastigera* (N) *I. pedicellaris* (O) *I. purga* (P) *I. santillani* Scale Bars: 2cm. All images taken by the author from material at the Missouri Botanical Garden Herbarium with permission from Dr. Jim Solomon, Curator.